Synthesis and Testing of Analogs of the Tuberculosis Drug Candidate SQ109 Against Bacteria and Protozoa: Identification of Lead Compounds Against *Mycobacterium abscessus* and Malaria Parasites

Marianna Stampolaki†,[1] Satish R. Malwal†,[2] Nadine Alvarez-Cabrera,[3] Zijun Gao,[2] Mohammad Moniruzzaman,[4] Svitlana O. Babii,[4] Nikolaos Naziris,[5] André Rey-Cibati,[6] Mariana Valladares-Delgado,[6] Andreea L. Turcu,[7] Kyung-Hwa Baek,[8] Trong-Nhat Phan,[8] Hyeryon Lee,[8] Mattheo Alcaraz,[9] Savannah Watson,[10] Mariette van der Watt,[10] Dina Coertzen,[10] Natasa Efstathiou,[1] Maria Chountoulesi,[5] Carolyn M. Shoen,[11] Ioannis P. Papanastasiou,[1] Jose Brea,[12] Michael H. Cynamon[11] Lyn-Marié Birkholtz,[10] Laurent Kremer, [9,13] Joo Hwan No,[8] Santiago Vázquez,[7] Gustavo Benaim,[6] Costas Demetzos,[5] Helen I. Zgurskaya, [4] Thomas Dick, [3,14,15] Eric Oldfield, [2]* Antonios D. Kolocouris [1]*

[1] Laboratory of Medicinal Chemistry, Section of Pharmaceutical Chemistry, Department of Pharmacy, National and Kapodistrian University of Athens, Panepistimiopolis-Zografou, Athens 15771, Greece

[2] Department of Chemistry, University of Illinois at Urbana–Champaign, Urbana, Illinois 61801, USA

[3] Center for Discovery and Innovation, Hackensack Meridian Health, Nutley, NJ 07110, USA

[4] University of Oklahoma, Department of Chemistry and Biochemistry, Stephenson Life Sciences Research Center, 101 Stephenson Parkway, Norman, OK 73019-5251, USA

[5] Section of Pharmaceutical Technology, Faculty of Pharmacy, National and Kapodistrian University of Athens, Panepistimiopolis-Zografou, Athens 15771, Greece

[6] Instituto de Estudios Avanzados, Caracas, Venezuela Instituto de Biología Experimental, Facultad de Ciencias, Universidad Central de Venezuela (UCV), Caracas, Venezuela

[7] Laboratori de Química Farmacèutica (Unitat Associada al CSIC), Departament de Farmacologia, Toxicologia i Química Terapèutica, Facultat de Farmàcia i Ciències de l'Alimentació, and Institute of Biomedicine (IBUB), Universitat de Barcelona, Av. Joan XXIII, 27-31, Barcelona, E-08028, Spain

[8] Host-Parasite Research Laboratory, Institut Pasteur Korea, Seongnam-si, Republic of Korea

[9] Institut de Recherche en Infectiologie de Montpellier, CNRS UMR9004, Université de Montpellier, 1919 route de Mende, 34293, Montpellier, France.

[10] Department of Biochemistry, Genetics and Microbiology, Institute for Sustainable Malaria Control, University of Pretoria, Hatfield, Pretoria, 0028, South Africa

[11] Central New York Research Corporation, Veterans Affairs Medical Center, Syracuse, NY 13210, U

[12] Drug Screening Platform/Biofarma Research Group, CIMUS Research Center, Departamento de Farmacoloxía, Farmacia e Tecnoloxía Farmacéutica, University of Santiago de Compostela (USC), 15782 Santiago de Compostela, Spain

[13] INSERM, IRIM, Montpellier, France

[14] Department of Medical Sciences, Hackensack Meridian School of Medicine, Nutley, NJ 07110, USA

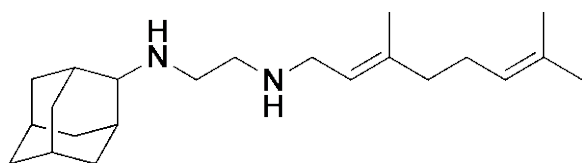[15] Department of Microbiology and Immunology, Georgetown University, Washington, DC 20007, USA

ABSTRACT

SQ109 is a tuberculosis drug candidate that has high potency against *Mycobacterium tuberculosis* and is thought to function at least in part by blocking cell wall biosynthesis by inhibiting the MmpL3 transporter. It also has activity against bacteria and protozoan parasites that lack MmpL3, where it can act as an uncoupler, targeting lipid membranes and Ca^{2+} homeostasis. Here, we synthesized 19 analogs of SQ109 and tested them against bacteria: *M. smegmatis*, *M. tuberculosis*, *M. abscessus*, *Bacillus subtilis* and *Escherichia coli*, as well as against the protozoan parasites, *Trypanosoma brucei*, *T. cruzi*, *Leishmania donovani*, *L. mexicana* and *Plasmodium falciparum*. Activity against the mycobacteria was generally less than with SQ109 and was reduced by increasing the size of the alkyl adduct, but two analogs were ~4-8 fold more active than was SQ109 against *M. abscessus*, including a highly drug resistant strain harboring a A309P mutation in MmpL3. There was also better activity than found with SQ109 with other bacteria and protozoa. Of particular interest, we found that the adamantyl C-2 ethyl, butyl, phenyl and benzyl analogs had 4-10x increased activity against *P. falciparum* asexual blood stages, together with low toxicity to a human HepG2 cell line, making them of interest as new anti-malarial drug leads. We also used surface plasmon resonance to investigate the binding of inhibitors to MmpL3, and differential scanning calorimetry to investigate binding to lipid membranes. There was no correlation between MmpL3 binding and *M. tuberculosis* or *M. smegmatis* cell activity, suggesting that MmpL3 is not a major target, in mycobacteria. However, some of the more active species decreased lipid phase transition temperatures, indicating increased accumulation in membranes, expected to lead to enhanced uncoupler activity.

2

INTRODUCTION

In 2020, an estimated 1.9 million people died from tuberculosis (TB), according to the World Health Organization. [1] Treatment with combinations of antibiotics (isoniazid, rifampicin, pyrazinamide, ethambutol) for six months can cure most people under optimal conditions, but globally, cure rates are less than optimal due to poor patient compliance to long-term chemotherapy, and the fact that some *Mycobacterium tuberculosis* (*Mtb*) strains have acquired mutations that render them resistant to many antibiotics. [2, 3] There is, therefore, the need for new, potent anti-tubercular drugs that have low rates of resistance. [2] One such drug candidate is the *N*-geranyl-*N'*-(2-adamantyl)ethane-1,2-diamine SQ109, [4] a second generation ethylenediamine which has been in phase II clinical trials [5, 6] and shows high potency against drug resistant *Mtb*. [7] SQ109 binds [8] to the trehalose monomycolate transporter, Mycobacterial membrane protein Large 3 (MmpL3), and is known to inhibit cell wall biosynthesis. MmpL3 transporter activity is driven by the proton motive force (PMF) and previous research has suggested that SQ109 can function by directly blocking the transporter's pore [9, 10] or indirectly, [7, 11] by acting as an uncoupler. Importantly, SQ109 also has a growth inhibitory activity against other bacteria [12, 13] (e.g. *Helicobacter pylori* [33,18]), fungi (e.g. *Candida albicans* [11]), malaria parasites (e.g. *Plasmodium falciparum*), [14] and the trypanosomatid parasite *Trypanosoma cruzi*, [15] all of which lack the MmpL3 transporter, or at least close homologs. There is, therefore, interest in the synthesis and testing of SQ109 analogs since these might have enhanced activity against not only mycobacteria, but also against other bacteria as well as against protozoa, yeasts and fungi.

Here, we synthesized a series of analogs of SQ109 containing alkyl, aryl or heteroaryl groups at the C2-adamantyl position (Figure 1). Then, we tested SQ109 and the analogs against the following mycobacteria: *M. smegmatis*, *M. tuberculosis* HN878*, M. tuberculosis* Erdman (MtErdman)*, M. tuberculosis* H37Rv (MtH37Rv), and *M. abscessus*. In addition, we tested these analogs against *Bacillus subtilis*, *Escherichia coli*, *Plasmodium falciparum* asexual blood stages*,* human hepatocyte carcinoma cells, *T. brucei* bloodstream forms, *T. cruzi* epimastigotes and amastigotes and their U20S host cells*, L. donovani* promastigote and *L. mexicana* promastigotes*.* We also explored the interaction of SQ109 and its analogs against MmpL3 using surface plasmon resonance (SPR), in addition to using differential scanning calorimetry (DSC) to explore the interactions of a subset of compounds with lipid bilayer membranes.

3

RESULTS AND DISCUSSION

Synthesis of SQ109 analogs. Based on the observation that the X-ray structure of SQ109 bound to MmpL3 [9] has the adamantyl group located close to four aromatic rings, we elected to synthesize a series of analogs with substituents at the adamantyl C-2 position which we reasoned might have enhanced hydrophobic interactions with the protein, as well as with membranes. For the synthesis of compounds **8b-i, 12** we used as starting material geranylamine (**2**), [16, 17] which we prepared from geraniol (**1**) using the Mitsunobu reaction (phthalimide, PPh₃, DEAD), and amines **5a-h**, **9a,** which we synthesized as described previously [18-20] (Figure 1). We carried out the preparation of the alcohol **5i** from the reaction of the 2-thiazolyl lithium reagents (generated from **3** [21, 22] with n-BuLi) and 2-adamantanone. We prepared the bromoacetamide (Figure 1) with Thz-Ph group **6i** as well as **10**, through a modified [20] Ritter reaction (BrCH₂CN, AcOH, H₂SO₄) from the corresponding tertiary alcohols **5i, 9b**. [18-20] We prepared the bromoacetamide derivatives **6a-h** and aminoacetamides **7b-c, 11** or **14b-h**, **15** as previously described for SQ109 (**8a**). [22] In aminoamides **14a-h**, **15** or **7a-i, 11**, compared to SQ109 (**8a**), it seemed possible that the bulkier substituents at the adamantyl C-2 carbon might hinder reduction of the amide carbonyl, leading to a mixture of the desired ethylenediamines, accompanied by amine decomposition by-products, formed when LiAlH₄ in THF is used. [23-25] We thus synthesized the amide precursors **7a-i, 11** or **14a-h**, **15** using LiAlH₄ in combination with freshly distilled trimethylchlorosilane (Me₃SiCl), in THF, with stirring for 2.5h at 0-10 °C under an argon atmosphere, as described for SQ109 (**8a**). [22] We obtained the diamines **8a-i**, **12** which were purified by using column chromatography, and were then converted to crystalline difumarate salts for cell growth inhibition testing. Aminoacetamides were tested as crystalline monofumarate salts.

Figure 1. Reagents and conditions: (a) Phthalimide, PPh$_3$, DEAD, and THF, rt, 24h (81%); (b) N$_2$H$_4$·H$_2$O, EtOH, reflux, 6h; (81%); (c) (i) n-BuLi, THF, -75 ^{o}C, 30 min; (ii) 2-adamantanone, THF, -75 ^{o}C, 1h; (iii) H$_2$O, 0 ^{o}C, (56%). (d$_i$) ClCOCH$_2$Br, K$_2$CO$_3$ (aq), CH$_2$Cl$_2$, rt, 24h (83-93%); (d$_{ii}$) BrCH$_2$CN, AcOH, H$_2$SO$_4$, rt, 1h (61%-quant.); (e) geranylamine (**2**), Et$_3$N, dry THF, rt, 48h (86-90%); (f) (i) Me$_3$SiCl, LiAlH$_4$, dry CH$_2$Cl$_2$, 0-5°C, Ar, 2.5 h; (ii) NaOH 10%, 0°C (20-40%).

Anti-bacterial and anti-protozoal activity of SQ109 analogs. We next investigated the activity of SQ109 (**8a**), its ethylenediamine analogs **8b-i, 12** and several aminoamide analogs: **7a, 7c, 7e, 7g, 7h, 14a, 14b, 14d, 11, 15** (Figure 1) against several bacteria, as well as protozoan parasites. We measured IC_{50} or MIC values (Table 1) against the following bacteria: *M. smegmatis*, *M. tuberculosis* HN878 (a virulent clinical strain), MtErdman, MtH37Rv, *M. abscessus*, *B. subtilis* and *E. coli*. The protozoa were *T. brucei* bloodstream forms, *T. cruzi* Dm28c epimastigotes and intracellular amastigotes (together with results for the U2OS host cells), *L. donovani* promastigotes, *L. mexicana* promastigotes and *P. falciparum* asexual bloodstream forms (ABS). For the protozoa, we determined parasite IC_{50} and EC_{50} values, as well as CC_{50} values for host cells. Results are shown in Tables 2 and 3.

We first screened the 19 SQ109 analogs (together with SQ109) against *M. smegmatis* (Table 1). The IC_{50} value for SQ109 (**8a**) against *M. smegmatis* was 2.4 µM, in good accord with previous work. [26] Addition of an n-butyl group at C-2 (**8e**) yielded essentially the same result (IC_{50} = 2.5 µM, Table 1) while shorter as well as more bulky substituents had less activity. For example, methyl (**8b**), ethyl (**8c**), n-propyl (**8d**), n-hexyl (**8f**), phenyl (**8h**) and benzyl (**8g**) group analogs had IC_{50} values in the ~4-6 µM range. The larger substituted thiazole (**8i**) was even less active, with IC_{50} = 20 µM (Table 1). Likewise, the C-1 substituted analog **12,** containing a dimethylmethylene group, was less active, with an IC_{50} value of 15 µM. Thus, the most active compounds have a relatively small substituent at C-2 and have IC_{50} values in the ~2-4 µM range. We then investigated the activity of SQ109 and the SQ109 analogs against MtHN878, a hypervirulent *M. tuberculosis* strain. Representative dose-response curves are shown in Figure 2a. MIC values are also shown in Table 1 and a correlation (R^2=0.96) between the log IC_{50} values from the dose response curves and the log MIC values from visual inspection is shown in Figure 2b. MIC value determination using visual inspection rather than a plate reader is particularly important with *M. abscessus*, described below, since in the rough (R) form cells are prone to clumping. As can be seen
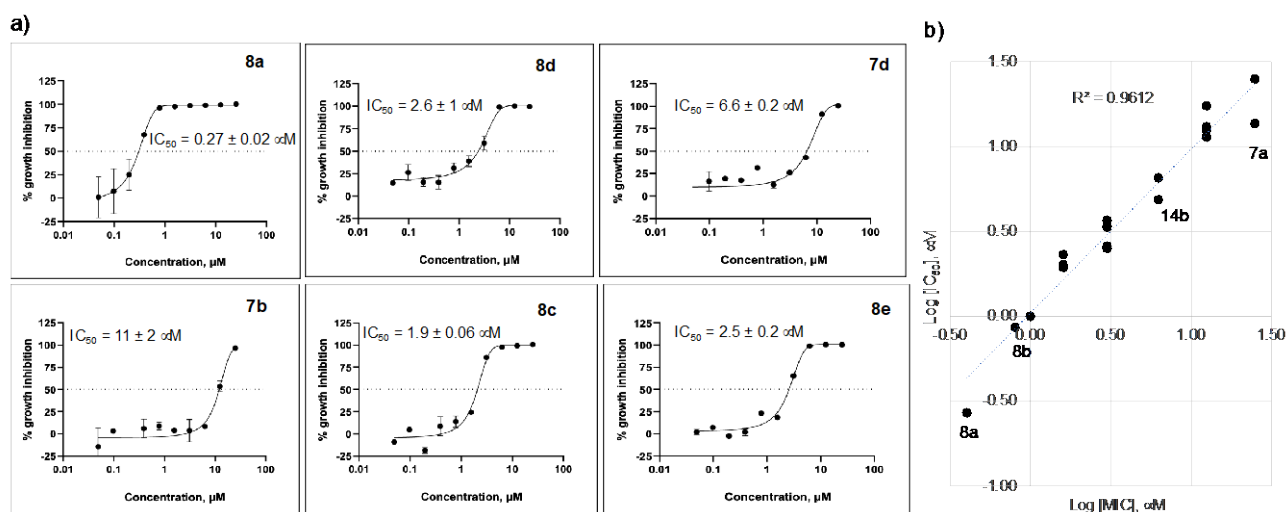
Figure 2. Dose-response curves for SQ109 and the SQ109 analogs against MtHN878 and correlation between log IC_{50} and log MIC values. a) Representative dose response curves. b) Correlation between log IC_{50} and log MIC values (R^2 = 0.9612).

in Table 1, the presence of a methyl group at C-2 (**8b**) yielded an IC_{50} = 0.86 µM (Table 1) which is ~3-fold higher than the IC_{50} = 0.27 µM of SQ109. The larger alkyl adducts, e.g. ethyl (**8c**), n-propyl (**8d**), n-butyl (**8e**), n-hexyl (**8f**), benzyl (**8g**) and phenyl (**8h**) analogs showed comparable IC_{50} values, in the ~2-3 µM range. In addition, we tested compounds against the *M. tuberculosis* Erdman and H37Rv strains, finding generally similar patterns of activity with the methyl adduct yielding an IC_{50} = 2 µM (Table 1) and other analogs with alkyl groups having IC_{50} values in the 4-8 µM range (Table 1). This activity was at least 2-fold lower than found with SQ109 (**8a**) (IC_{50} = 1 µM), and the aminoamides (**7a, 7c, 7e, 7g 7h, 14a, 14b, 14d, 11, 15**) were generally less active than the more basic, ethylenediamine analogs.

In addition to investigating *M. tuberculosis*, we also investigated activity against *M. abscessus*, which is increasingly recognized [27] as an emerging opportunistic pathogen causing severe lung disease, particularly in cystic fibrosis patients. Since it is intrinsically resistant to most conventional antibiotics, there is an unmet need for effective treatments.[27] We determined the *in vitro* activity of SQ109 and a series of analogs against both smooth (S) and rough (R) variants of *M. abscessus*, which differ in their susceptibility profile to several antibiotics. As has been shown previously, [6] the MIC of SQ109 (**8a**) was much higher against *M. abscessus* (here, 22-44 µM) than against *M. tuberculosis* (~0.3-1 µM). However, the n-butyl analog **8e** as well as the benzyl analog **8g** had significantly improved activity against both the S and R variants (MICs of 5.8-6.2 µM), warranting future work on benzyl derivatives. The MIC values of all compounds against the R and S strains were either identical to or within a factor of 2x of each other. We also investigated an *M. abscessus* strain harboring a

A309P mutation located in the transmembrane domain in MmpL3 (strain PIPD1[R1]), which displays very high resistance to the piperidinol-containing molecule PIPD1, [28] the indole-2 carboxamide Cpd12, [25] and the benzimidazole EJMCh-6. [25] Surprisingly, this mutant was not resistant to SQ109 or its analogs, having essentially the same MIC values as the wild type strains. This is a potentially important observation since resistance to other MmpL3 inhibitors can be very large (e.g. 32-64x for PIPD1[28]). This lack of resistance may indicate that binding to MmpL3 is not the primary target of SQ109 (**8a**) and its analogs, in *M. abscessus*.

We then questioned whether any of the compounds investigated had activity against other bacteria, ones which lack MmpL3. In the gram-positive bacterium *B. subtilis*, SQ109 (**8a**) had an IC_{50} value of 16 µM (Table 1) and of interest, several of the SQ109 analogs had much better activity. For example, n-butyl (**8e**), n-hexyl (**8f**) and phenyl (**8h**) analogs had IC_{50} values in the 0.5 -1.0 µM range (Table 1). We also observed that some tested aminoamides had activity, in the 2-5 µM range. In the gram-negative bacterium *E. coli*, the IC_{50} value for SQ109 (**8a**) was 15 µM and the n-alkyl (propyl, butyl, hexyl) analogs had IC_{50} values in the ~ 8-10 µM range—slightly better than found with SQ109 (**8a**). Since neither *B. subtilis* nor *E. coli* contain the MmpL3 protein, other targets must be involved, so the promising activity of some compounds is of interest, for future work. There was either no inhibition or very low inhibition (IC_{50} values > 70 µM) with the aminoamides tested (Table 1), suggesting that the ethylenediamine group might play a role in activity, as an uncoupler—as previously suggested for *Mtb* and protozoa.

Next, we investigated the activities of the SQ109 analogs against the following protozoa: *T. brucei*, *T. cruzi*, and two *Leishmania* species. In each case, the activity of SQ109 (**8a**) against these protozoa has been reported previously and has been proposed to arise from protonophore uncoupling, as well as effects on Ca^{2+} homeostasis. [15, 29, 30] Results for SQ109 (**8a**) and the analogs are shown in Table 2 and representative dose-response curves are shown in Figure S1. With *T. brucei* bloodstream forms, SQ109 (**8a**) had an IC_{50} value of 0.91 µM and slightly better activity was found with the adamantyl C-2 n-propyl (**8d**), n-butyl (**8e**), n-hexyl (**8f**) and benzyl (**8g**) analogs (IC_{50} values of 0.88 µM, 0.37 µM, 0.98 µM and 0.85 µM, respectively), but is slightly less with phenyl (**8h**) and C-1 dimethylmethylene (**12**) analogs (IC_{50} values of 1.3 µM, 1.4 µM, respectively). Of interest, the aminoamides also had activity although IC_{50} values were ~5-10-fold larger (in the range ~ 2-12 µM) compared to the ethylenediamines (**8b-g, 12**). With *T. cruzi*, we investigated both the epimastigotes as well as the (clinically relevant) amastigote forms, and activity against the host cell (U2OS). With epimastigotes, the IC_{50} of SQ109 was 6.8 µM which is ~3-4x larger than that found with the C2 ethylene diamine analogs, n-propyl (**8d**), n-butyl (**8e**) and the C-1 dimethylmethylene analog (**12**). With aminoamide
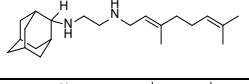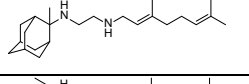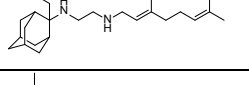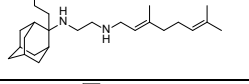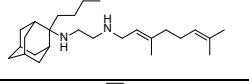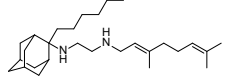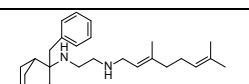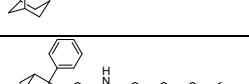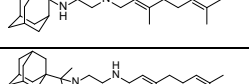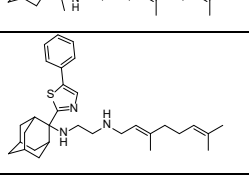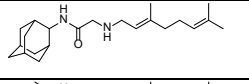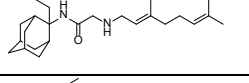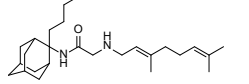
analogs, activity was again lower than with the ethylene diamine analogs. With the intracellular amastigote form, SQ109 (**8a**) had an IC_{50} value of 0.74 μM and all of the ethylenediamine analogs had good activity, with the phenyl (**8h**) analog being comparable to (though not clearly b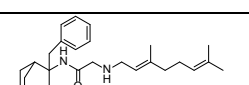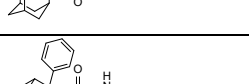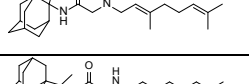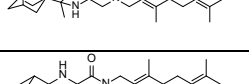etter than) SQ109**.** The aminoamides were all less active, with IC_{50} values in the range ~ 2-9 μM. The same trends in activity were seen with the inhibition of host cell growth, with the ethylenediamines being more potent host cell growth inhibitors than were the amides. With *L. donovani*, we tested SQ109 and 18 analogs (Table 2). The IC_{50} value for SQ109 was 2 μM and the adamantyl C-2 methyl (**8b**), ethyl (**8c**), n-propyl (**8d**), n-butyl (**8e**), phenyl (**8h**), dimethylmethylene (**12**) analogs had higher or similar activity (in the 1-4 μM range), while the n-hexyl (**8f**) analog was less active (IC_{50} = 8.8 μM) as was the benzyl (**8g**) analog (IC_{50} = 6.1 μM). As with *T. brucei* and *T. cruzi*, the aminoamides were in general less (or much less) active with IC_{50} values in the range ~ 5-44 μM. With *L. mexicana* the IC_{50} value for SQ109 (**8a**) was 0.50 μM and the adamantyl C-2 methyl (**8b**) had an IC_{50} = 0.43 μM while the n-propyl (**8d**) was ~4-fold less active (IC_{50} = 1.94 μM). Several aminoamides had similar activity with **8d** and amide **14d** having IC_{50} = 0.73 μM (Table 2).
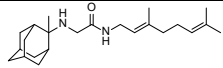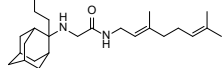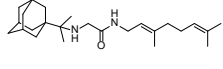
In addition to investigating the trypanosomatid parasites, we also investigated the asexual bloodstream form of the apicomplexan parasite *P. falciparum* (PfABS). As previously reported, [26] SQ109 (**8a**) has activity against the PfABS parasite and only modest toxicity against HepG2 (human hepatocellular carcinoma) cells. We thus evaluated SQ109 and 13 of its analogs finding more potent (~100-900 nM) PfABS activity with the adamantyl C-2 methyl (**8b**), ethyl (**8c**), n-propyl (**8d**), n-butyl (**8e**), phenyl (**8h**) and benzyl (**8g**) analogs, as well as with the C-1 dimethylmethylene analog (**12**), compared to SQ109 (IC_{50} = 1.6 μM, Table 3). The ethyl (**8c**) analog had ~10-fold better activity than that obtained with SQ109 (160 nM versus 1.6 μM), while the phenyl (**8h**) and benzyl (**8g**) analogs had 4x and 5x increased potency, respectively. Using HepG2 cell line viability as a test of overt toxicity, we found that there was 43% cell viability at 20 μM with the ethyl analog, but 100% viability with both phenyl and benzyl analogs, making them of potential interest as an antimalarial hit with low toxicity against mammalian cells.

When taken together, the results with *M. tuberculosis* cell growth inhibition indicate that it is difficult to improve upon the activity of SQ109 (**8a**) by adding substituents at the C-2 position. For example, the methyl (**8b**) and benzyl (**8g**) substituents at the adamantyl C-2 group had ~2-4-fold less activity against MtbHN878, MtErdman and MtH37Rv (Table 1). However, there was promising activity against both the S and R variants of *M. abscessus.* What is also of course of interest is the observation that some of the analogs do have better activity that does SQ109 against bacteria that lack the putative MmpL3 target, e.g. *B. subtilis* and *E. coli*, as also found with the malaria parasite, *P.*

falciparum. A question then arises as to whether there is any correlation between MmpL3 binding and cell activity, in the mycobacteria.
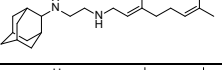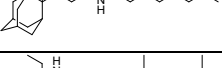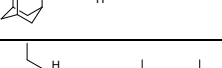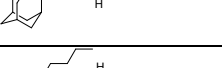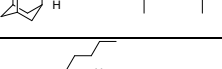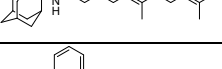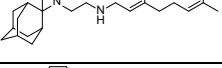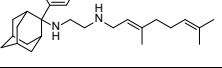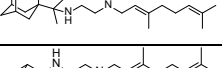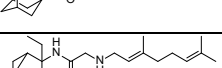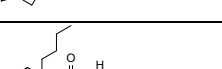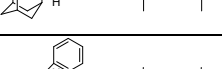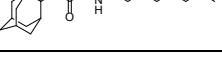
Table 1. **Anti-bacterial activity of SQ109 analogs.**

Comp. No	Chemical structure	*Ms* IC$_{50}$ (µM)	*Mtb* HN878 IC$_{50}$ (µM)	*Mtb* HN878 MIC (µM)	*Mtb* Erdman MIC (µM)	*Mtb* H37Rv MIC (µM)	*Ma*(S) MIC (µM)	*Ma*(R) MIC (µM)	*Bs* IC$_{50}$ (µM)	*Ec* IC$_{50}$ (µM)
8a		2.4 ± 0.3	0.27 ± 0.02	0.4	1.8	1.8	44	22	16	15
8b		4.4 ± 0.5	0.86 ± 0.06	0.8	3.5	3.5	43	22	ND	25
8c		4.0	1.9 ± 0.06	1.6	6.8	6.8	22	10.7	4.3	18
8d		4.3 ± 0.8	2.6 ± 1	3	13	13	10	10	ND	7.6
8e		2.5	2.5 ± 0.2	3	9.7	12.9	6.2	6.2	0.54	7.8
8f		4.7	3.4 ± 0.6	3	12	12	12	12	1.0	9.2
8g		6.0	2.0 ± 0.5	1.6	6.1	6.1	5.8	5.8	0.59	1.3 x 10^2
8h		5.8	2.3 ± 0.2	1.6	13	13	12	6	ND	No inhibition
12		15 ± 2	3.4 ± 0.6	3	13	13	12.9	12.9	ND	8.9
8i		21	ND	ND	ND	ND	21.5	21.5	ND	ND
7a		45 ± 6	>25	25	340	340	ND	ND	ND	2.3 x 10^2
7c		7.7	6.6 ± 0.2	6.25	16	16	ND	ND	1.9	No inhibition
7e		17	13 ± 0.3	12.5	15	15	ND	ND	2.8	No inhibition
7g		17	11 ± 1	12.5	29	29	ND	ND	2.3	No inhibition
7h		26	ND	ND	38	38	ND	ND	4.5	No inhibition
11		44 ± 4	13 ± 2	12.5	19	19	ND	ND	ND	No inhibition
14a		5 ± 0.8	3.7 ± 0.6	3	16	21	ND	ND	ND	695

Comp No	Chemical structure								
14b		9	4.9 ± 0.1	6.25	20	30	ND	ND	ND	No inhibition
14d		49 ± 5	>25	25	32	32	ND	ND	ND	No inhibition
15		31 ± 3	17 ± 6	12.5	38	38	ND	ND	ND	No inhibition

Abbreviations used: *Ms*, *M. smegmatis*; *Mtb*, *M. tuberculosis*; *Ma*, *M. abscessus*; S, smooth variant; R, rough variant; *Bs*, *Bacillus subtilis*; *Ec*, *E. coli*. ND=not determined.

Table 2. **Activity of SQ109 analogs against Trypanosomatid parasites**

Comp. No	Chemical structure	*T. brucei* IC_{50} µM	*T. cruzi*			*L. donovani* IC_{50} µM	*L. mexicana* IC_{50} (µM)
			IC_{50} (EPI) µM	IC_{50} (PAR) µM	CC_{50} (U2OS) µM		
8a		0.91 ± 0.03	6.8 ± 2	0.74 ± 0.04	4.1 ± 0.2	2.0 ± 0.1	0.73 ± 0.2
8b		2.1 ± 0.02	3.5 ± 1	0.77 ± 0.2	2.8 ± 0.7	2.0 ±1	0.43 ± 0.08
8c		1.4 ± 0.2	8.0 ± 2	1.3 ± 0.06	2.5 ± 0.3	2.1 ± 0.4	ND
8d		0.88 ± 0.2	2.1 ± 0.9	0.60 ± 0.5	1.6 ± 0.1	2.0 ±0.2	1.9 ± 0.2
8e		0.37 ± 0.02	2.5 ± 1	0.84 ± 0.5	1.7 ± 1	4.0 ± 0.4	ND
8f		0.98 ± 0.09	8.2 ± 0.4	1.3 ± 0.07	4.1 ± 1	8.8 ± 0.4	ND
8g		0.85 ± 0.09	6.6 ± 1	0.92 ± 0.06	2.0 ± 0.4	6.1 ± 0.06	ND
8h		1.3 ± 0.3	7.3 ± 2	0.60 ± 0.04	3.5 ± 1	1.4 ± 1	ND
12		1.4 ± 0.03	2.4 ± 0.7	0.56 ± 0.9	1.4 ± 0.2	2.3 ± 0.1	4.7 ± 0.2
7a		12 ± 1	>100	4.2 ± 0.4	14 ± 0.7	10 ± 0.5	2.2 ± 0.8
7c		3.9 ± 0.3	14 ± 0.04	3.2 ± 0.2	7.5 ± 0.6	44 ± 11	ND
7e		3.0 ± 0.2	48 ± 0.07	8.8 ± 1.3	15 ± 0.5	25 ± 14	ND
7g		5.6 ± 1	17 ± 4	2.9 ± 0.3	7.0 ± 0.2	27 ± 0.8	ND
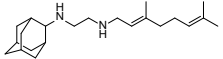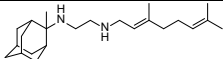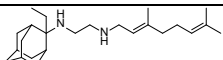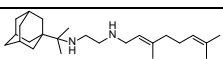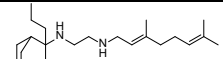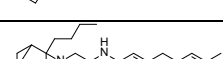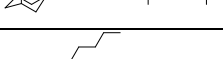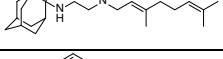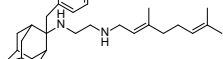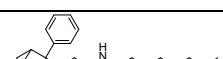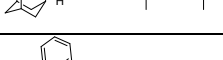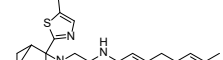
Comp. No	Chemical structure						
7h		4.1 ± 0.6	18 ± 2	3.4 ± 0.2	7.0 ± 0.4	26 ± 28	ND
11		6.2 ± 0.2	16 ± 4	4.4 ± 0.3	6.9 ± 0.1	5.0 ± 0.6	5.2 ± 0.2
14a		9.9 ± 0.7	28 ± 4	2.7 ± 0.2	9.5 ± 0.9	12 ± 0.9	2.0 ± 0.2
14b		6.6 ± 0.03	18 ± 4	2.3 ± 0.2	7.2 ± 0.9	11 ± 0.9	2.4 ± 0.7
14d		2.3 ± 0.1	14 ± 5	2.8 ± 0.3	9.1 ± 0.4	8.4 ± 2	0.73 ± 0.2
15		5.9 ± 0.1	15 ± 3	2.6 ± 0.1	7.1 ± 0.5	12 ± 8	5.0 ± 0.1
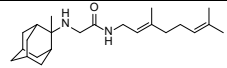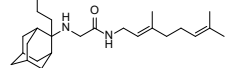
Table 3. Activity of SQ109 analogs against *Plasmodium falciparum* asexual blood stages

Comp. No	Chemical structure	PfABS IC$_{50}$ (μM ± S.E.)	HepG2 % viability @ 20 μM
8a		1.58 ± 0.2	97
8b		0.66 ± 0.18	100
8c		0.16 ± 0.07	43 (85% @ 2 μM)
8d		0.53 ± 0.22	100
8e		0.27 ± 0.04	50 (83% @ 2 μM)
8g		.032 ± 0.03	100
8h		0.42 ± 0.09	100
7a		6.49 ± 0.33	100
11		7.63 ± 1.13	100
12		0.77 ± 0.1	100
14a		>10	99
14b		6.47 ± 0.65	94
14d		5.27 ± 0.41	100
15		5.44 ± 0.32	76 (91% @ 2 μM)

MmpL3–inhibitor binding interactions. We next used SPR to investigate the binding of SQ109 and several analogs to an expressed *M. tuberculosis* MmpL3 (MtMmpL3).[10] We focused on measurement of the K_D values for SQ109 (**8a**) and the 9 ethylenediamine analogs **8b-i, 12,** together with four aminoamides **7a**, **14a**, **14b**, and **14d**. The experimental SPR results are shown in Figure S2. Data were fit using the two-state model, as described previously, [10] together with the 1:1 binding model. The rate constants and the equilibrium dissociation constants K_D for both models are shown in Tables 4 and 5. The two-state binding model that postulates a conformational change in the protein upon binding of an inhibitor gave improved statistical fits as seen from lower residuals values. However, as can be seen in Table 4 there are essentially no differences between the K_D values obtained using either model.
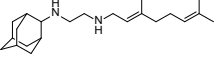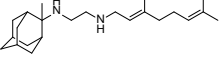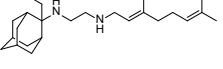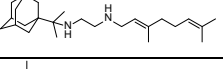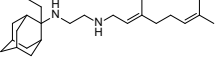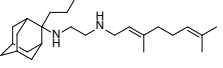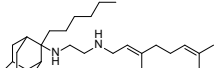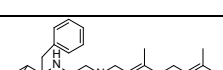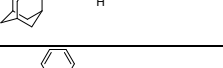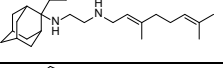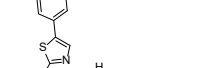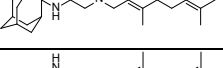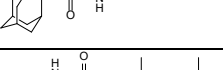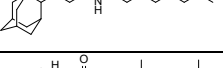
Table 4. SPR results *for M. tuberculosis* **MmpL3-ligand binding using a 1:1 binding model**[a]

Comp. No	Chemical structure	k_{on} ($1/_{M \times s}$)	k_{off} ($1/_s$)	K_D, µM 1:1 model	Residuals χ^2 (RU)^2
8a		351.9	0.882	2510	58.7
8b		3658	0.6882	188	16
8c		4710	0.8409	180	37.9
12		6276	0.6646	106	62.2
8d		5926	0.5403	91	48.9
8e		3998	0.3888	97	22.6
8f		4441	0.2964	67	126
8g		5789	0.3999	69	85.1
8h		4060	0.465	115	110
8i		5627	0.4902	87	108
7a		9.44E+02	0.236	250	19.4
14a		4537	1.27	280	10.7

14b		1762	0.7506	426	44.1
14d		3.00E+03	0.754	252	24.2

[a],Data were fit globally using the 1:1 Langmuir binding model. Equilibrium dissociation constants (K_D) were calculated from the ratio of the dissociation and association rate constants.

Table 5. SPR results *for M. tuberculosis* MmpL3-ligand binding using the 2-state model[a]

Comp. No	Chemical structure	k_{a1} ($1/{M \times s}$)	k_{d1} ($1/s$)	k_{a2} ($1/s$)	k_{d2} ($1/s$)	K_D, µM 2-state	Residuals χ^2 (RU)^2
8a		429.8	1.098	0.005315	0.02222	2060	34.5
8b		4958	1.613	0.01084	0.03486	248	9.52
8c		5473	1.284	0.006994	0.03012	190	7.57
12		7245	1.05	0.007539	0.03558	120	15
8d		7325	0.9488	0.00968	0.04246	106	12.2
8e		5151	0.7008	0.009897	0.03763	108	7.48
8f		4642	0.4552	0.008637	0.03992	81	38.9
8g		6462	0.5715	0.006528	0.03248	74	30.3
8h		2.59E+04	4.085	0.00526	0.03247	136	29.5
8i		3946	0.434	0.006253	0.03057	91	31.1
7a		1.23E+04	4.816	0.01065	0.04928	321	4.38
14a		2345	2.023	0.009004	0.02642	644	4.18
14b		1917	1.363	0.009268	0.02741	531	12.6
14d		3277	1.04	0.005907	0.03103	267	9.59

What has been puzzling about the SPR result for SQ109 binding to *M. tuberculosis* MmpL3 (MtMmpL3) reported previously is that the K_D value for SQ109 (**8a**) was high, ~ 1.5 mM, while the IC_{50} against *M. tuberculosis* itself ($IC_{50} \approx$ 0.4-1 µM, Table 1) is very low. The IC_{50} for *M. smegmatis* (Table 1) is higher, ~2.4 µM, but again much lower that the K_D value measured against MtMmpL3 (Table 4). The K_D values for all 14 compounds tested are lower than found with SQ109 (**8a**) (Tables 4 and 5). What is of particular interest is that, compared to SQ109 (**8a**), there is a general decrease in the K_D value, meaning tighter binding to MmpL3, as the compounds become more hydrophobic. For example, using the K_D values from the two-state binding model that are shown in Table 5, with SQ109 (**8a**) and the adamantyl C-2 substituted species (see structure of R in Scheme 1) we found the following K_D values R=H (**8a** or SQ109, 2060 µM); R=methyl (**8b**, 248 µM); R=ethyl (**8c**, 190 µM); R=n-propyl (**8d**, 106 µM); R=n-butyl (**8e**, 108 µM); R=n-hexyl (**8f**, 81 µM). That is, as the R substituent at C-2 (which is an H in SQ109) becomes larger and more hydrophobic, the K_D decreased. A similar effect was observed with phenyl (**8h**, 136 µM) and benzyl (**8g**, 74 µM) C-2 substituents (Table 5). The C-1 dimethylmethylene analog **12** had a K_D of 106 µM, which was close to the isomeric C-2 n-propyl **8d** which had a K_D of 120 µM. The thiazole **8i** was also a relatively good binder with K_D ~90 µM (Table 4).

As can be seen in Figure 3a, there is a significant correlation between the log K_D values for all 14 compounds (i.e. including the four amides) and $logD_{7.4}$, the computed oil-water partition coefficient at pH=7.4, with a Pearson R coefficient R=0.73 and p<0.003. That is, the strongest binding occurs with the most hydrophobic species. This is not unexpected, however, we find no correlation between cell growth inhibition and log K_D, Figure 3b, or between cell growth inhibition and $logD_{7.4}$, for all of the compounds tested, Figure 3c. Essentially the same results were obtained using either the 1:1 or 2-state models for K_D.
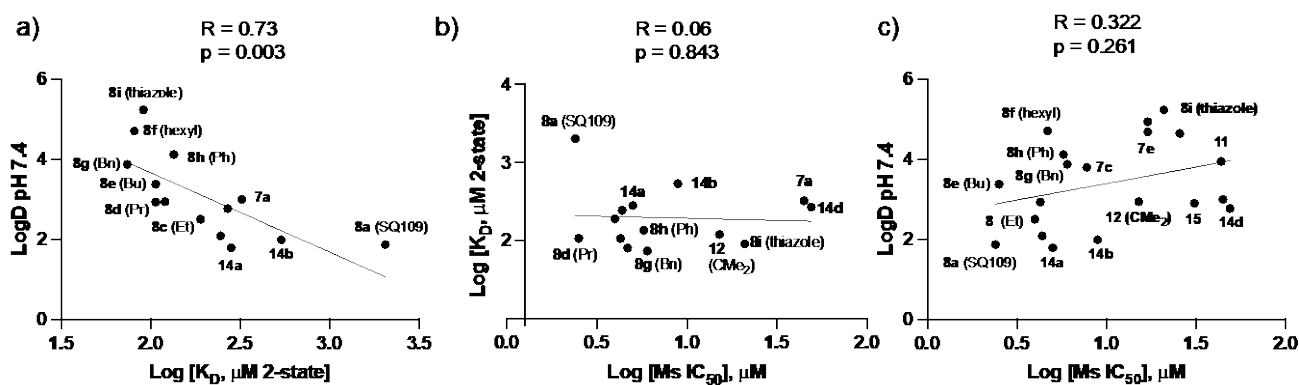
Figure 3. Graphs showing correlations between log K_D, $LogD_{7.4}$ and *M. smegmatis* cell growth inhibition. (a) Log K_D versus $logD_{7.4}$; R=0.73, p=0.003. (b) Log Ms IC_{50} and log K_D; R=0.06, p=0.843 (c) Log Ms IC_{50} and $logD_{7.4}$, for all compounds tested; R=0.322, p=0.261. Selected compound numbers are shown.

One possible reason for this is that while the more hydrophobic species **8b-i, 12** do bind more strongly to MmpL3 compared to SQ109 (**8a**), there may be unfavorable steric interactions with the highly glycosylated mycobacterial cell wall with the larger substituents, [31, 32] or with any transporters that may facilitate cell entry. It is also of course possible that there may be other targets such as MenA, MenG, involved in menaquinone biosynthesis, which could contribute to the observed differences in activities. [23] The activity of other proteins may also be targeted, together with binding to lipid membranes, affecting uncoupling activity and the proton motive force, as well as affecting lipid membrane inhibitor-concentrations (and thus, activity). The importance of steric effects in influencing poor cell uptake in the mycobacteria seems likely since as can be seen in Table 1 and Figure 3, the bulky adamantyl C-2 phenylthiazoyl (**8i**) analog—while exhibiting stronger binding to MmpL3 than does SQ109 (**8a**) —had only very weak activity against *M. smegmatis* cell growth. With *M. tuberculosis* HN878, where full dose-response curves were obtained, there was a similar trend, with SQ109 (**8a**) being most active (IC_{50} = 0.4 μM), followed by the C-2 Me analog **8b** (IC_{50} = 0.8 μM), the ethyl analog **8c** (IC_{50} = 1.6 μM), n-propyl (**8d** and n-hexyl (**8f**) analogs both having IC_{50} = 3 μM. In *M. tuberculosis* HN878, the phenyl (**8h**) and benzyl (**8g**) analogs had the same activity, IC_{50} = 1.6 μM. Overall then, the SPR results do not support the idea that MmpL3 is the major target for SQ109 (**8a**) or analog activity in the mycobacteria, meaning that other targets such as uncoupling activity, or indeed other mechanisms of action, are involved, consistent of course with the activity (for SQ109) seen against other bacteria, as well as against yeasts, fungi and protozoa.

Membrane–inhibitor interactions. Another target for SQ109 (**8a**) in both bacteria and protozoa involves effects on the proton motive force, and Ca^{2+} homeostasis—both of which involve cell membranes. In previous work [33] we investigated the pH dependence of the activity of inhibitors, including SQ109 analogs, on *M. smegmatis* cell growth inhibition (IC_{50} values) and found that there were correlations between the IC_{50} values and uncoupling (ΔpH collapse), as well as with changes in the gel-to-liquid crystal phase transition temperature (T_m) in DSC experiments with lipid bilayer membranes, and with computed logD values. We showed [33] that cell growth inhibition activity increased from pH 5 to 7 to 9, and this correlated with increasing uncoupler activity, decreasing T_m values, and increasing logD values. That is, increased hydrophobicity results in more membrane binding leading to more fluidity and uncoupling activity, as well as providing a reservoir of inhibitor for binding to membrane protein targets. Such effects could be important in the protozoa.

We therefore next used DSC to investigate the effects of SQ109 (**8a**) and analogs **8b-g, 12** on the gel-to-liquid crystal phase transition in 1,2-dimyristoyl-sn-glycero-3-phosphocholine (DMPC) bilayers (10 wt % inhibitor, pH 7.4) as well as with 1,2-distearoyl-sn-glycero-3-phosphoglycerol (DSPG) bilayers. The zwitterionic DMPC is a model for protozoal membranes which are primarily phosphatidylcholines and phosphatidylethanolamines, while the DSPG is an anionic species and is a model for the mycobacterial inner membrane lipids. DSC scans of each compound during heating (Figures 4a,b, Table 6) and cooling (Figure S3, S4, Table S1) were then compared with measurements on DMPC or DSPG alone. The DSC scans of the main transition for the DMPC systems (Figure 4a) showed that compared to DMPC without any inhibitor, SQ109 (**8a**), **12** decreased T_m by 3-4 °C, while **8b** (Me), **8c** (Et), **8d** (Pr), **8e** (Bu), **8f** (Hex), **8g** (Bn) and **8h** (Ph) decreased T_m by ca. 5.6, 6.6, 6, 7.8, 9.7, 6.9 and 8.8 °C, respectively (Table 6). The DSC scans for DSPG systems in Figure 4b showed that compared to DSPG alone SQ109 (**8a**), **8b** (Me), **12** and **8d** (Pr) decreased the T_m by 3-4 °C, while **8e** (Bu), **8f** (Hex), **8g** (Bn) and **8h** (Ph) decreased T_m by ~5 °C (Table 6).
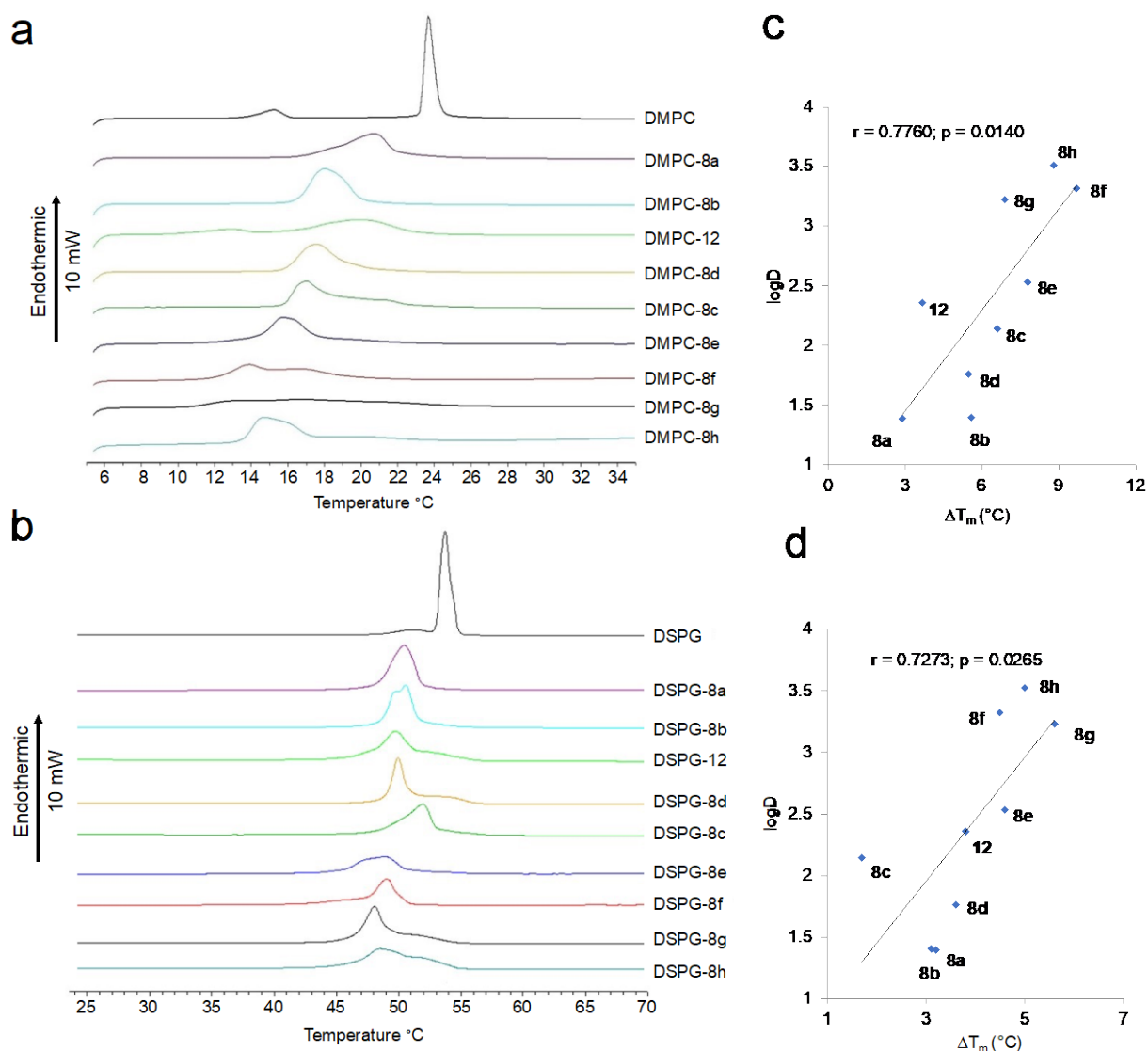
Figure 4. DSC results for DMPC and DSPG with and without SQ109 (**8a**) and 8 ethylenediamine analogs and correlations between ΔT_m and $logD_{7.4}$. (a) DSC heating scans for DMPC. (b) DSC heating scans for DSPG. (c) Correlation between $logD_{7.4}$ and the decrease in T_m (ΔT_m) for DMPC. Pearson r-coefficient = 0.776, p = 0.014. (d) as in (c) but for DSPG. Pearson r-coefficient = 0.727, p = 0.026.

These results indicated that SQ109 (**8a**) and the analogs incorporate into the phospholipid bilayers and fluidize the membranes, generating a structure that melts at a lower temperature, T_m, compared to the pure membrane, and this effect was more pronounced as the size of the inhibitor increases. Compared to the pure DMPC bilayer, SQ109 (**8a**) or **8b** (Me), **8c** (Et), **8d** (Pr), **8e** (Bu), **8h** (Ph), **12** broadened the main transition peak by $\Delta T_{1/2}$ = 0.7-2.4 °C (Table 6), while compounds **12**, **8f** (Hex) and **8g** (Bn) broadened by $\Delta T_{1/2}$ = 3.5, 4.4, 9.6 °C, due most likely to the formation of inhomogeneous domains that melt over a broad temperature range. Similarly, compared to the pure DSPG bilayer, SQ109 (**8a**), **8b** (Me), **8c** (Et), **8d** (Pr), **8f** (Hex), **8g** (Bn) and **12** broadened the main transition peak by $\Delta T_{1/2}$ = 0.2-1.6 °C; while compounds **8e** (Bu) and **8h** (Ph) broadened the peak by 2.7 and 4.4 °C,

respectively, again due most likely to the formation of inhomogeneous domains that melt over a broad temperature range.[34] However, rather than simply a very large broadening of the gel-to-liquid crystal phase transition, as seen with the fluidizing effect of cholesterol,[35] in all cases T_m shifted to lower temperatures. The DSC thermograms obtained on cooling, Figure S3, S4 and Table S1, showed a similar decrease in T_m as seen with DMPC on heating but a more complex hysteresis effect with DSPG.

What is perhaps surprising is that, in general, the effects on T_m seen with DPMC were clearly larger than those seen with DSPG. What might the reasons for this be? Interestingly, similar effects have been reported for the binding of another cationic antibiotic, the anthracycline pirarubicin [36] binding to DSPG and to distearoylphosphatidylcholine (DSPC), in which the acyl chain lengths are the same (C_{18}). In that work [36] it was proposed (based on the results of DSC, Fourier transform infra-red spectroscopy and quantum chemical calculations) that the ammonium group of the antibiotic bound more tightly to the PO_2^- group in DSPG than to the PO_2^- group in DSPC, due to charge repulsion with the choline Me_3N^+ group in DSPC, and that this resulted in decreased drug incorporation into the lipid bilayer. These observations led us to the following model for SQ109-DMPC/DSPG interactions. First, incorporation of the SQ109 geranyl (C_{10}) chain into the lipid bilayer was expected to decrease T_m in the same way that incorporation of a farnesyl (C_{15}) group in farnesol [37] decreased and broadened the DMPC main transition, due to disrupted packing of the DMPC alkyl chains. A similar effect would be predicted for both DMPC as well as DSPG, but the effect would be larger with the shorter chain species, DMPC, which has a similar alkyl chain length to that of the geranyl chain in SQ109. The enthalpy of the phase transition was also of course much larger with the longer chain, DSPG, species, Table 6. However, there is a second interaction that may also be of importance, the electrostatic interaction between the PO_2^- group in the phospholipid and the protonated ethylenediamine group of SQ109 (**8a**) (or analog). Binding of cationic species (e.g. Ca^{2+}, UO_2^{2+}) to anionic lipids increases T_m [38] and it is possible that SQ109 (**8a**) may help "cross-link" the anionic DSPG, thereby off-setting to some extent the fluidizing effect of the geranyl group in SQ109 (**8a**).

Table 6. DSC results (heating) for the DMPC:SQ109 analog systems in DMPC hydrated with PBS (phosphate buffered saline, pH=7.4) and calculated $logD_{7.4}$ values at the same pH.

Sample	T_m	$\Delta T_{1/2}$	ΔH	Sample	T_m	$\Delta T_{1/2}$	ΔH	$logD_{7.4}$
DMPC	23.5	0.59	30.3	DSPG	53.6	0.9	48.1	
DMPC:**8a** (H)	20.6	2.6	23.3	DSPG:**8a** (H)	50.4	2.1	54.0	1.39
DMPC:**8b** (Me)	17.9	2.2	25.6	DSPG:**8b** (Me)	50.5	2.0	53.2	1.40
DMPC:**12**	19.8	4.1	17.8	DSPG:**12**	49.8	2.4	55.8	2.36
DMPC:**8d** (Pr)	17.5	2.2	22.6	DSPG:**8d** (Pr)	50.0	1.1	48.1	2.14
DMPC:**8c** (Et)	16.9	2.0	24.0	DSPG:**8c** (Et)	51.9	2.5	49.9	1.76
DMPC:**8e** (Bu)	15.7	2.2	24.4	DSPG:**8e** (Bu)	49.0	3.6	38.5	2.53
DMPC:**8f** (Hex)	13.8	5.1	24.6	DSPG:**8f** (Hex)	49.1	1.7	36.6	3.32
DMPC:**8g** (Bn)	16.6	10	21.6	DSPG:**8g** (Bn)	48.0	1.7	55.5	3.23
DMPC: **8h** (Ph)	14.7	2.7	29.8	DSPG: **8h** (Ph)	48.6	5.3	55.4	3.52

m: main transition; T_m (°C), temperature at which heat capacity (ΔC_P) at constant pressure is a maximum; $\Delta T_{1/2}$ (°C), half width at half peak height of the main transition; ΔH (kJ mol^{-1}), main transition enthalpy normalized per g of the bilayer. Results were the same after two repeats.

What is also of particular interest about the DSC results shown in Figure 4a,b is that there are good correlations between the change in T_m that correlates with the computed $logD_{7.4}$ of the inhibitor, Figures 3c and 3d, with a Pearson r-coefficient = 0.776, p = 0.014 for DMPC and a Pearson r-coefficient = 0.727, p = 0.026 for DSPG. For the cooling curves, there was again a correlation between ΔT_m and logD with DMPC (r = 0.75, p = 0.021) but there were more complex effects with DSPG (Figure S4). The stronger binding of the more hydrophobic analogs to lipid membranes would be expected to result in more cell activity, either by increasing membrane fluidity/uncoupling activity or by providing higher membrane concentrations for a membrane protein target. However, the more hydrophobic analogs were not found to be more active against *M. tuberculosis* or *M. smegmatis*, but we did find increased activity (a 4-8 fold decrease in MIC) in *M. abscessuss*, as well as large increases in activity against *B. subtilis* and *E. coli*, Table 1, and with *P. falciparum* (with the phenyl and benzyl analogs). The DSC results thus suggest that the larger analogs may simply not reach their target(s) in *M. tuberculosis* and *M. smegmatis*, e.g. due to unfavorable steric interactions with the mycolyl-arabinogalactan-peptidoglycan cell wall.

Microsomal stability and solubility. Finally, we investigated the microsomal stability of analog **8b** (Me) and analog **8h** (Ph) as well as of SQ109 (**8a**) in human, mice and rat liver microsomes. In previous work, Jia et al,[39, 40] found that SQ109 was metabolized in rats, mice, and dogs with [^{14}C- SQ109] half-life values of 5 h in mice[39] and >5 h in rats and dogs[40]. Using liver microsomes and cells expressing P450 enzymes, they concluded that SQ109 was rapidly metabolized to oxygenated species, and we recently reported their structures[26]. It was thus of interest to investigate whether SQ109 analogs were also metabolized, using liver microsome assays. We found that, as expected [39, 40] SQ109 (**8a**) was rapidly metabolized (Table S2), while the methyl analog **8b** was ~2-4x more stable (% remanent at 60 minutes) than was SQ109 (**8a**). The phenyl analog **8h** had the same % remanent as SQ109 (**8a**) (at 60 minutes) in mice microsomes, though was more rapidly metabolized in human and rat liver microsomes. The intrinsic clearance rates (CL$_{int}$) in mice microsomes were essentially the same as found with SQ109 for **8b** and **8h** but were about twice as large as found with SQ109 (**8a**) in the human and rat liver microsome assays (Table S2). While all of these rates are high, it is of course well known that SQ109 (**8a**) is, nevertheless, effective against *M. tuberculosis* in humans where it accumulates in the lungs, and in addition, it has efficacy against both trypanosomatid as well as apicomplexan parasites, in mice models of infection, [41] where the lungs are not targeted. Clearly, it will be of interest to determine how e.g. **8h** is metabolized, and whether any metabolites have activity, and further work on this topic as well as on the synthesis of **8h** analogs, is of interest. To determine the susceptibility of the phenyl group in **8h** to oxygenation we used 3 computer programs: the GloryFame2 program,[42, 43] the Xenosite program[44] and the SmartCyp program.[45] Results are shown in Figure S5. Based on these results it is apparent that in general the major sites targeted by P450 cytochromes are—as with SQ109 (**8a**) itself— at the ends of the molecule (the terminal methyl groups and the adamantyl group) and at C10, but the phenyl group is also a potential target and may form a phenol (C19, Figure S5a, GloryFame2 result; Figure S5c, SmartCyp result) or a quinone (Figure S5b) moiety.

CONCLUSIONS

In this work we report the synthesis of analogs of the anti-tubercular drug candidate SQ109 (**8a**), an ethylenediamine-based inhibitor of MmpL3 currently undergoing clinical trials that also has activity against a broad range of bacteria, protozoa and even some yeasts/fungi. We synthesized a series of 19 SQ109 (**8a)** analogs containing adamantane C-2 alkyl, aryl or heteroaryl adamantyl groups (Me, Et, Pr, Bu, Ph, Bn, Hex, 4-phenylthiazol-2-yl**,** with ethylenediamine or aminoamide linkers between the adamantyl and geranyl groups, in addition to an adamantyl C-1 dimethylmethylene

analog. We then tested SQ109 (**8a**) and the analogs against five bacteria: *M. smegmatis*, *M. tuberculosis* (3 strains), *M. abscessus* (two strains), *B. subtilis* and *E. coli*, as well as against five protozoa, *T. brucei*, *T. cruzi* (epimastigotes and amastigotes), *L. donovani*, *L. mexicana* and *P. falciparum* (asexual blood stages). There was good activity of ethylenediamine analogs containing small substituents against the mycobacteria, though activity was generally less than with the SQ109 parent molecule. The interesting exception was in *M. abscessus* where we found two SQ109 analogs, the butyl (**8e**) and benzyl (**8g**) species, in which activity was ~4-8 fold higher than found with SQ109 (**8a**). Moreover, activity was the same against a highly drug-resistant *M. abscessus* strain, harboring a A309P mutation located in the transmembrane domain in MmpL3, indicating that MmpL3 is not a major target in this species. We then used SPR to investigate the binding of SQ109, nine ethylenediamine analogs and four amide analogs to a mycobacterial MmpL3 protein target finding that tighter MmpL3 binding correlated with increasing ligand hydrophobicity with r=0.73, p<0.003 for the $logK_D/logD_{7.4}$ correlation. However, there were no significant correlations between cell growth inhibition and either logD or $logK_D$. The low activity of the more potent MmpL3 binders against MmpL3-containing bacteria suggests that MmpL3 inhibitors with large C-2 substituents may not be able to penetrate the cell wall. Using DSC, we found that these inhibitors caused larger decreases in T_m than found with SQ109 (**8a**), indicating efficient accumulation in lipid membranes and there were clear correlations between ΔT_m and $logD_{7.4}$ for both DMPC (r = 0.776, p = 0.014) as well as for DSPG (r = 0.727, p = 0.026). Taken together, the SPR and DSC results are consistent with the idea that the larger, more potent MmpL3 inhibitors are less effective than is SQ109 (**8a**) in penetrating the arabinogalactan-peptidoglycan cell wall in mycobacteria. In contrast, in *B. subtilis* and *E. coli*, several analogs were more potent than was SQ109 (**8a**). In these organisms, MmpL3 is absent as is the mycolyl-arabinogalactan-peptidoglycan cell wall, although the mechanism of action of SQ109 (**8a**) itself in these bacteria remains to reported. On the other hand, in the trypanosomatid parasites, SQ109 (**8a**) is reported to act as a protonophore uncoupler that also affects Ca^{2+} homeostasis. In these organisms there is again no cell wall, and many of the analogs are active against the parasites. With the malaria parasite *P. falciparum*, there is likewise no cell wall and no MmpL3 and SQ109 and analog activity could similarly be dependent on their protonophore properties. We found that several analogs had 4-10x increased activity over SQ109 as well as low toxicity against the HepG2 human cell line making them of interest as a new anti-malarial drug hit, warranting further development of these more-bulky analogs, as antimalarial drug leads*.*

METHODS

22

General. All solvents and chemicals were used as purchased without further purification except for Me₃SiCl which was distilled just before use. Dry ether and dry dichloromethane were prepared by leaving the solvents over CaH_2 for 24 h before use. Anhydrous THF was purchased in sealed bottles from Acros Organics. The progress of all reactions was monitored on Merck precoated silica gel plates (with fluorescence indicator UV254) using diethyl ether/n-hexane, n-hexane/ethyl acetate or chloroform/methanol as eluents. Column chromatography was performed with Acros Organics silica gel 60A 40-60 μm with the solvent mixtures described in the experiment section. Compounds' spots were visualized based on their absorbance at 254 nm. The structures of **8a-i, 12** were identified using ¹H, ¹³C and LC-MS. High-resolution mass spectrometry (HRMS) was carried using a UHR-TOF maXis 4G instrument (Bruker Daltonics, Bremen, Germany). ¹H NMR spectra were recorded in CDCl₃ solutions for the amines and CD₃OD solutions for the fumarate salts of amines on Bruker NMR spectrometers, the DRX 200 or DRX 400 or DRX 600 at 200 MHz or 400 or 600 MHz, respectively; ¹³C NMR spectra were recorded at 50 MHz, 100 or 150 MHz, respectively. Carbon multiplicities were assigned using the DEPT experiment. 2D NMR HMQC and COSY spectra were used for the elucidation of the structures of intermediates and final products and NMR peaks assignments. All compounds were confirmed to have greater than 95% purity via HPLC-MS analysis. We described [22] an improved preparation of geranylamine (**2**) and the preparation of **6a, 7a, 13, 14a, 8a** was also reported in ref [22]; the preparation of geranylamine (**2**) and the raw materials for amines **5b-h, 12** were the corresponding adamantanols obtained from the reaction of 2-amantanone with alkyl lithium reagents. The tertiary alcohols were then reacted with a mixture of sodium azide and trifluoroacetic acid in dichloromethane and the produced tertiary alkyl azides were reduced with LiAlH₄ in ether at rt to afford the amines **5b-h, 12**. [18, 20] The 2-adamantylamine **5a** was prepared from reduction of 2-adamantanone oxime with LiAlH₄ in THF. The preparation of intermediates **2, 5i, 6a-i, 10, 13** and of **7a**, **14a** and SQ109 (**8a**) published in ref [22] can be found in the Supporting Information.

2-((3,7-Dimethylocta-2,6-dien-1-yl)amino)-N-(2-methyl-2-adamantanyl)acetamide, **7b**
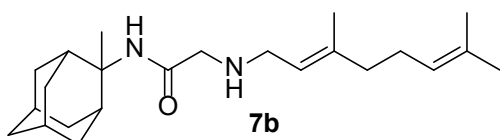
Bromoacetamide **6b** (660 mg, 2.31 mmol) in dry THF (13 mL) was added dropwise at 0 °C to a stirred mixture of geranylamine (**2**) (353 mg**,** 2.31 mmol) and triethylamine (233 mg, 2.31 mmol) in dry THF

23

(20 mL). The stirring continued for 48 h at room temperature. Then the aqueous phase was extracted twice with dichloromethane, the combined organic extracts were evaporated in vacuo and the crude product was purified through column chromatography using a. ether:n-hexane (1:1), b. CHCl$_3$:MeOH (9:1), as eluents. Acetamide **7b** was obtained as a pale yellow oil; yield 744 mg (90%); ^{1}H-NMR (CDCl$_3$, 400 MHz) δ (ppm) 1.51 (s, 3H, 2-adamantyl-CH$_3$), 1.59 (s, 3H, 8-geranyl), 1.64 (s, 3H, 7-geranyl CH$_3$), 1.67 (s, 3H, 3-geranyl CH$_3$), 1.80 (s, 2H, 5,7-adamantyl), 1.96-2.05 (m, 6H, 4,5-H, 8ax,10ax-adamantyl), 2.18 (d, J = 12 Hz, 2H, 4ax,9ax-adamantyl) 3.17 (d, J = 7.4 Hz, 2H, 1-geranyl) 3.28-3.30 (m, 2H, COC<u>H</u>$_2$NH), 5.07 (m, 1H, 6-geranyl), 5.23 (m, 1H, 2-geranyl); ^{13}C-NMR (CDCl$_3$, 100MHz) δ (ppm) 16.7 (3-geranyl CH$_3$), 18.1 (8-geranyl), 23.5 (2-adamantyl-CH$_3$), 26.0 (7- geranyl CH$_3$), 27.2 (5-geranyl), 27.2 (5-adamantyl), 27.8 (7-adamantyl), 33.6 (4,9-adamantyl), 35.7 (1,3-adamantyl), 38.9 (8,10-adamantyl), 39.9 (6-adamantyl), 40.1 (4-geranyl), 47.3 (1-geranyl), 58.5 (2-adamantyl), 59.7 (CO<u>C</u>H$_2$NH), 123.1 (2-geranyl), 124.1 (6-geranyl), 132.2 (7-geranyl), 138.5 (3-geranyl), 168.9 (C=O); HRMS (ESI-TOF (+)) m/z [M + H]$^+$ calculated for [C$_{23}$H$_{39}$N$_2$O]$^+$ 359.3057, found 359.3062.

N-(3,7-dimethylocta-2,6-dien-1-yl)-N´-(2-methyl-2-adamantanyl)ethane-1,2-diamine, **8b**

8b
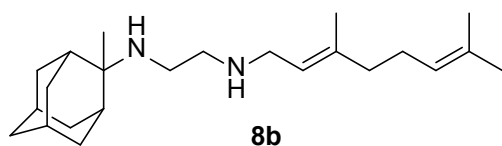
Acetamide **7b** (790 mg, 2.21 mmol) in dry dichloromethane (10 mL) was stirred at 0-5 ℃ for 15 min under argon atmosphere. Recently distilled trimethylsilyl chloride (288 µL, 2.65 mmol) was then added at the same temperature and the mixture was stirred for another 15 min. A suspension of LiAlH$_4$ (117 mg, 3.09 mmol) in a small quantity of THF was added at -10-0°C and the stirring continued for 2.5 h at the same temperature. The mixture was then treated with NaOH 10%, the resulting inorganic precipitate was filtered off, the organic phase was separated and the aqueous phase was extracted twice with dichloromethane. The combined organic extracts were evaporated in vacuo and the crude product was dissolved in dichloromethane and washed with brine. After the evaporation of the solvent, the crude product was purified through column chromatography using a. CHCl$_3$:MeOH (9:1), b. CHCl$_3$:MeOH:NH$_3$ (88:10:2), as system solvents to afford diamine **8b** as a pale yellow oil; yield 190 mg (25%); ^{1}H-NMR (CDCl$_3$, 400 MHz) δ (ppm) 1.21 (s, 3H, 2-adamantyl-CH$_3$), 1.51 (d, J = 12Hz, 2H, 4eq,9eq-adamantyl), 1.53 (s, 2H, 8eq,10eq-adamantyl), 1.59 (s, 3H, 8-geranyl), 1.63 (s, 3H, 7-geranyl CH$_3$), 1.67 (s, 3H, 3-geranyl CH$_3$), 1.80 (d, J = 12Hz, 2H, 5,7-adamantyl), 1.98-2.12 (m, 4H, 4,5-geranyl),

2.64 (t, *J* = 6Hz, 2H, NHC<u>H</u>₂CH₂NH-geranyl), 2.74 (t, *J* = 6Hz, 2H, NHCH₂C<u>H</u>₂NH-geranyl), 3.23 (d, *J* = 7.0 Hz, 2H, 1-geranyl), 5.09 (m, 1H, 6-geranyl), 5.25 (m, 1H, 2-geranyl); ¹³C NMR (CDCl₃, 100MHz) *δ* (ppm) 16.6 (3-geranyl CH₃), 18.0 (8-geranyl), 23.2 (2-adamantyl CH₃), 26.0 (7-adamanytyl CH₃), 26.9 (5-geranyl), 27.5 (5-adamantyl), 28.4 (7-adamantyl), 32.9 (4,9-adamantyl), 34.5 (1,3-adamantyl), 36.3 (8,10-adamantyl), 39.3 (6-adamantyl), 40.0 (4-geranyl), 40.2 (1-geranyl), 47.4 (NH<u>C</u>H₂CH₂NH-geranyl), 50.1 (NHCH₂<u>C</u>H₂NH-geranyl), 56.3 (2-adamantyl), 123.3 (2-geranyl), 124.5 (6-geranyl), 131.8 (7-geranyl), 138.0 (3-geranyl); HRMS (ESI-TOF (+)) *m/z* [M + H]⁺ calculated for [C₂₃H₄₁N₂]⁺ 345.3264, found 345.3269; Purity of the product determined by HPLC-MS: 96.4%.

N-(3,7-dimethylocta-2,6-dien-1-yl)-2-((2-methyl-2-adamantanyl)amino)acetamide, **14b**
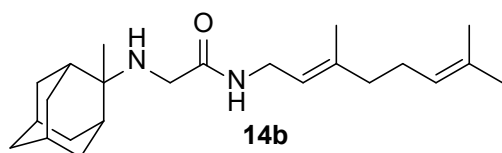
Bromoacetamide **13** (664 mg, 2.42 mmol) in dry THF (14 mL) was added dropwise at 0 °C to a stirred solution of 2-methyl-2-adamantanamine (**5b**) (400 mg**,** 2.42 mmol) and triethylamine (244 mg, 2.42 mmol) in dry THF (24 mL). The stirring continued for 48 h at room temperature. Then the aqueous phase was extracted twice with dichloromethane, the combined organic extracts were evaporated in vacuo and the crude product was purified through column chromatography using a. ether:n-hexane (1:1), b. CHCl₃:MeOH (9:1), as eluents. Acetamide **14b** was obtained as a yellow oil; yield 520 mg (60%); ¹H-NMR (CDCl₃, 400 MHz) *δ* (ppm) 1.14 (s, 3H, 2-adamantyl CH₃), 1.55 (d, *J* = 12Hz, 2H, 4eq,9eq-adamantyl), 1.59 (s, 3H, 8-geranyl), 1.67 (s, 6H, 3,7-geranyl CH₃), 1.91-1.94 (m, 2H, 4ax,9ax-adamantyl), 1.99-2.08 (m, 4H, 4,5-geranyl), 3.20 (s, 2H, NHC<u>H</u>₂CO), 3.86 (t, *J* = 6 Hz, 2H, 1-geranyl), 5.08 (m, 1H, 6-geranyl), 5.19 (m, 1H, 2-geranyl). Hydrochloride salt; ¹³C-NMR (CD₃OD, 100MHz,) *δ*(ppm) 17.2 (3-geranyl CH₃), 18.6 (8-geranyl), 21.4 (2-adamanyl CH₃), 26.7 (7-geranyl CH₃), 28.3 (5-geranyl), 28.4 (5-adamantyl), 29.1 (7-adamantyl), 33.4 (4,9-adamantyl), 35.4 (8,10-adamantyl), 36.1 (1,3-adamantyl), 39.6 (6-adamantyl), 39.9 (4-geranyl), 41.4 (1-C), 43.3 (NH<u>C</u>H₂CO), 67.3 (2-adamantyl), 121.3 (2-geranyl), 125.8 (6-geranyl), 133.5 (7-geranyl), 142.1 (3-geranyl), 167.1 (C=O); HRMS (ESI-TOF (+)) *m/z* [M + H]⁺ calculated for [C₂₃H₃₉N₂O]⁺ 359.3057, found 359.3057; Purity of the product determined by HPLC-MS: 98.0%.

N-(2-(adamantan-1-yl)propan-2-yl)-2-((3,7-dimethylocta-2,6-dien-1-yl)amino)acetamide, **11**

11
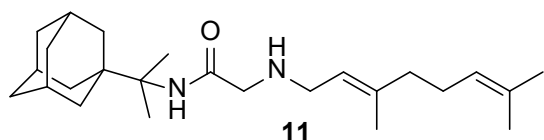
Bromoacetamide **10** (680 mg, 2.16 mmol) in dry THF (15 mL) was added dropwise at 0 °C to a stirred solution of geranylamine (**2**) (330 mg, 2.16 mmol) and triethylamine (218 mg, 2.16 mmol) in dry THF (20 mL). The stirring continued for 48 h at room temperature. Then the aqueous phase was extracted twice with dichloromethane, the combined organic extracts were evaporated in vacuo and the crude product was purified through column chromatography using a. ether:n-hexane (1:1), b. $CHCl_3$:MeOH (9:1), as eluents. Acetamide **11** was obtained as a yellow oil; yield 750 mg (90%); ^{1}H-NMR (CDCl$_3$, 400 MHz) δ (ppm) 1.34 (s, 6H, 1-adamantyl C(CH$_3$)$_2$), 1.59-1.71 (m, 21H, 2,4,6,8,9,10-adamantyl, 8-geranyl, 3,7-geranyl CH$_3$), 2.01-2.09 (m, 7H, 3,5,7-adamantyl, 4,5-geranyl), 3.15 (d, J = 7.4 Hz, 2H, 1-geranyl), 3.23-3.26 (m, 2H, COCH$_2$NH), 5.07 (m, 1H, 6-geranyl), 5.22 (m, 1H, 2-geranyl); ^{13}C-NMR (CDCl$_3$, 100MHz) δ(ppm) 16.7 (3-geranyl CH$_3$), 18.0 (8-geranyl), 21.4 (1-adamanyl C(CH$_3$)$_2$), 21.9 (1-adamantyl C(CH$_3$)$_2$), 26.0 (7-geranyl CH$_3$), 26.8 (5-geranyl), 28.9 (3,5,7-adamantyl C), 36.5 (4,6,10-adamantyl), 37.4 (2,8,9-adamantanyl), 39.5 (1-adamantanyl), 39.8 (4-geranyl), 40.0 (1-geranyl), 47.3 (COCH$_2$NH), 59.01 (1-adamanyl C(CH$_3$)$_2$), 119.8 (2-geranyl), 124.2 (6-geranyl), 132.1 (7-geranyl), 140.4 (3-geranyl), 169.1 (C=O); HRMS (ESI-TOF (+)) m/z [M + H]$^+$ calculated for [C$_{25}$H$_{43}$N$_2$O]$^+$ 387.337, found 387.337; Purity of the product determined by HPLC-MS: 99.2%.

N-(3,7-dimethylocta-2,6-dien-1-yl)-N´-(2-(adamantan-1-yl)propan-2-yl)ethane-1,2-diamine, **12**

12
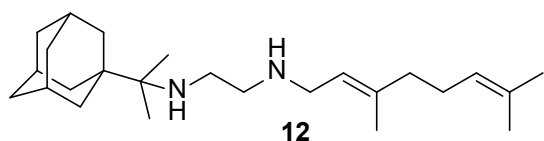
Acetamide **11** (280 mg, 0.72 mmol) in dry dichloromethane (4 mL) was stirred at 0-5 °C for 15 min under argon atmosphere of Ar. Recently distilled trimethylsilyl chloride (94 µL, 0.87 mmol) was then added at the same temperature and the mixture was stirred for another 15 min. A suspension of LiAlH$_4$ (38.3 mg, 1.01 mmol) in a small quantity of THF was added at -10-0°C and the stirring continued for 2.5 h at the same temperature. The mixture was treated with NaOH 10%, the resulting inorganic precipitate was filtered off, the organic phase was separated and the aqueous phase was extracted twice with dichloromethane. The combined organic extracts were evaporated in vacuo and the crude

product was dissolved in dichloromethane and washed with brine. After the evaporation of the solvent, the crude product was purified through column chromatography using a. CHCl$_3$:MeOH (9:1), b. CHCl$_3$:MeOH:NH$_3$ (88:10:2), as system solvents, to afford diamine **12** as a yellow oil; yield 70mg (26%); ^{1}H-NMR (CDCl$_3$, 400 MHz) δ (ppm) 0.96 (s, 6H, 1-adamantyl C(CH$_3$)$_2$), 1.60-1.67 (m, 21H, 2,4,6,8,9,10-adamantane H, 8-geranyl, 3,7-geranyl CH$_3$), 2.01-2.09 (m, 7H, 3,5,7-adamantyl, 4,5-geranyl), 2.70 (s, 4H, NHCH$_2$CH$_2$NH), 3.23 (d, J = 7.0 Hz, 2H, 1-geranyl), 5.09 (m, 1H, 6-geranyl), 5.26 (m, 1H, 2-geranyl); ^{13}C NMR (CDCl$_3$, 100MHz) δ(ppm) 16.6 (3-geranyl CH$_3$), 18.0 (8-geranyl), 20.7 (1-adamantyl C(CH$_3$)$_2$), 26.0 (7-geranyl CH$_3$), 26.9 (5-geranyl), 29.2 (3,7,5-adamantyl), 36.5 (4,6,10-adamantyl), 37.6 (2,8,9-adamantyl), 39.2 (1-adamantyl), 40.0 (4-geranyl), 41.9 (1-geranyl), 47.2 (NHCH$_2$CH$_2$NH-geranyl), 50.2 (NHCH$_2$CH$_2$NH-geranyl), 57.2 (1-adamantyl C(CH$_3$)$_2$), 123.0 (2-geranyl), 124.5 (6-geranyl), 131.9 (7-geranyl), 138.3 (3-geranyl); HRMS (ESI-TOF (+)) m/z [M + H]$^+$ calculated for [C$_{25}$H$_{45}$N$_2$]$^+$ 373.3577, found 373.357; Purity of the product determined by HPLC-MS: 96.6%.

2-((2-(Adamantan-1-yl)propan-2-yl)amino)-N-(3,7-dimethylocta-2,6-dien-1-yl)acetamide, **15**

15
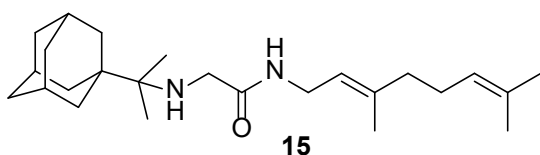
Bromoacetamide **13** (200 mg, 0.73 mmol) in dry THF (6 mL) was added dropwise at 0 °C to a stirred solution of 2-(1-adamantanyl)propan-2-amine (**9**) (141 mg, 0.73 mmol) and triethylamine (74 mg, 0.73 mmol) in dry THF (8 mL). The stirring continued for 48 h at room temperature. Then the aqueous phase was extracted twice with dichloromethane, the combined organic extracts were evaporated in vacuo and the crude product was purified through column chromatography using a. ether:n-hexane (1:1), b. CHCl$_3$:MeOH (9:1), as eluents. Acetamide **15** was obtained as a yellow oil; yield 125 mg (44%); ^{1}H-NMR (CDCl$_3$, 400 MHz) δ (ppm) 0.92 (s, 6H, 1-adamantyl C(CH$_3$)$_2$), 1.59-1.73 (m, 21H, 2,4,6,8,9,10-adamantyl, 8-geranyl, 3,7-geranyl CH$_3$), 2.01-2.10 (m, 7H, 3,5,7-adamantyl, 4,5-geranyl), 3.28 (s, 2H, NHCH$_2$CO), 3.85 (t, J = 6.2 Hz, 2H, 1-geranyl), 5.08 (m, 1H, 6-geranyl), 5.21 (m, 1H, 2-geranyl); ^{13}C-NMR (CDCl$_3$, 100MHz) δ(ppm) 16.7 (3-geranyl CH$_3$), 18.0 (8-geranyl), 20.3 (1-adamantyl C(CH$_3$)$_2$), 26.0 (7-geranyl CH$_3$), 26.9 (5-geranyl), 29.0 (3,5,7-adamantyl), 36.5 (4,6,10-adamantyl), 37.4 (2,8,9-adamantyl), 37.9 (1-adamantyl), 39.0 (4-geranyl), 39.8 (1-geranyl), 46.1 (NHCH$_2$CO), 120.3 (2-geranyl), 124.2 (6-geranyl), 132.0 (7-geranyl), 140.2 (3-geranyl), 169.2 (C=O); HRMS (ESI-TOF (+)) m/z

[M + H]$^+$ calculated for [C$_{25}$H$_{43}$N$_2$O]$^+$ 387.337, found 387.3369; Purity of the product determined by HPLC-MS: 95.8%.

*2-((3,7-Dimethylocta-2,6-dien-1-yl)amino)-N-(2-ethyladamantan-2-yl)acetamide,* **7c**

7c
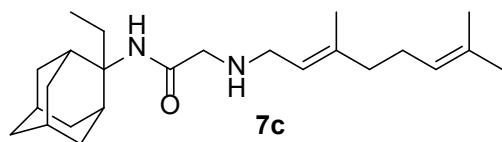
Bromoacetamide **6c** (680 mg, 2.26 mmol) in dry THF (15 mL) was added dropwise at 0 °C to a stirred solution of geranylamine (**2**) (346 mg, 2.26 mmol) and triethylamine (228 mg, 2.26 mmol) in dry THF (20 mL). The stirring continued for 48 h at room temperature. Then the aqueous phase was extracted twice with dichloromethane, the combined organic extracts were evaporated in vacuo and the crude product was purified through column chromatography using a. ether:n-hexane (1:1), b. CHCl$_3$:MeOH (9:1), as eluents. Acetamide **7c** was obtained as a pale yellow oil; yield 710 mg (84%); ^{1}H-NMR (CDCl$_3$, 400 MHz) δ (ppm) 0.75 (t, *J* = 7Hz, 3H, 2-adamantyl CH$_2$CH$_3$), 1.60 (s, 3H, 8-geranyl), 1.63 (s, 3H, 7-geranyl CH$_3$), 1.68 (s, 3H, 3-geranyl CH$_3$), 1.60-1.70 (m, 6H, 1,3,4eq,8eq,9eq,10eq-adamantyl), 1.81 (s, 2H, 6-adamantyl), 1.93-2.11 (m, 10H, 5,7,8ax,10ax-adamantyl, 2-adamanyl CH$_2$CH$_3$, 4,5-geranyl), 2.25 (s, 2H, 4ax,9ax-adamantyl), 3.19 (s, 2H, COCH$_2$NH), 3.23 (d, *J* = 7.4 Hz, 2H, 1-geranyl), 5.07 (t, *J* = 7.4 Hz, 1H, 6-geranyl), 5.20 (t, *J* = 7.4 Hz, 1H, 2-geranyl); ^{13}C-NMR (CDCl$_3$, 100MHz) δ (ppm) 7.43 (2-adamantyl CH$_2$CH$_3$), 16.6 (3-geranyl CH$_3$), 18.0 (8-geranyl C), 25.0 (2-adamantyl CH$_2$CH$_3$), 26.0 (7-geranyl CH$_3$), 26.8 (5-geranyl C), 27.6 (5,7-adamantyl), 33.2 (4,9-adamantyl), 33.1 (1,3-adamantyl), 33.7 (8,10-adamantyl), 39.0 (6-adamantyl), 40.0 (4-geranyl), 47.7 (1-geranyl), 52.7 (COCH$_2$NH), 60.4 (2-adamantyl), 122.2 (2-geranyl), 123.6 (6-geranyl), 132.1 (7-geranyl), 139.3 (3-geranyl), 170.3 (C=O); HRMS (ESI-TOF (+)) *m/z* [M + H]$^+$ calculated for [C$_{24}$H$_{41}$N$_2$O]$^+$ 373.3213, found 373.3213; Purity of the product determined by HPLC-MS: 99.2%.

N-(3,7-dimethylocta-2,6-dien-1-yl)-N'-(2-ethyladamantan-2-yl)ethane-1,2-diamine, **8c**

8c
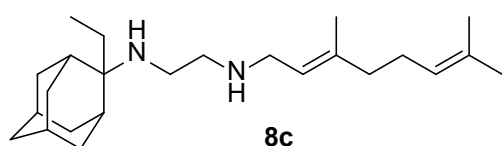
Acetamide **7c** (420 mg, 1.13 mmol) in dry dichloromethane (5 mL) was stirred at 0-5 °C for 15 min under argon atmosphere. Recently distilled trimethylsilyl chloride (147 µL, 1.35 mmol) was then added at the same temperature and the mixture was stirred for another 15 min. A suspension of LiAlH$_4$ (60 mg, 1.58 mmol) in a small quantity of THF was added at -10-0°C and the stirring continued for 2.5 h at the same temperature. The mixture was then treated with NaOH 10%, the resulting inorganic precipitate was filtered off, the organic phase was separated and the aqueous phase was extracted twice with dichloromethane. The combined organic extracts were evaporated in vacuo and the crude product was dissolved in dichloromethane and washed with brine. After evaporation of the solvent, the crude product was purified through column chromatography using a gradient of CHCl$_3$:MeOH (20:1, 18:1), as system solvents, to afford diamine **8c** as a pale yellow oil; yield 150 mg (37%); ^{1}H-NMR (CDCl$_3$, 400 MHz) δ (ppm) 0.75 (t, J = 7Hz, 3H, 2-adamantyl CH$_2$C$\underline{H}_3$), 1.48 (d, J = 12Hz, 2H, 4eq,9eq-adamantyl), 1.59 (s, 3H, 8-geranyl), 1.63 (s, 3H, 7-geranyl CH$_3$), 1.67 (s, 3H, 3-geranyl CH$_3$), 1.59-1.67 (m, 4H, 1,3,8eq,10eq-adamantyl), 1.80 (s, 2H, 6-adamantyl), 1.90 (d, J = 12 Hz, 2H, 5,7-adamantyl), 1.99-2.18 (m, 10H, 4ax,8ax,9ax,10ax-adamantyl, 2-adamantyl C$\underline{H}_2$CH$_3$, 4,5-H), 2.54 (t, J = 6Hz, 2H, NHC$\underline{H}_2$CH$_2$NH-geranyl), 2.74 (t, J = 6 Hz, 2H, NHCH$_2$C$\underline{H}_2$NH-geranyl), 3.26 (d, J = 7.0 Hz, 2H, 1-geranyl), 5.08 (t, J = 7 Hz, 1H, 6-geranyl), 5.26 (t, J = 7 Hz, 1H, 2-geranyl); ^{13}C NMR (CDCl$_3$, 100MHz) δ (ppm) 6.6 (2-adamantyl CH$_2$C$\underline{H}_3$), 16.6 (3-geranyl CH$_3$), 18.1 (8-geranyl), 24.0 (2-adamantyl C$\underline{H}_2$CH$_3$), 26.0 (7-geranyl CH$_3$), 26.8 (5-geranyl), 28.1 (5,7-adamantyl), 32.9 (4,9-adamantyl), 33.9 (1,3,8,10-adamantyl), 39.4 (6-adamantyl), 40.0 (1,4-geranyl), 47.2 (NHC$\underline{H}_2$CH$_2$NH-geranyl), 49.9 (NHCH$_2$C$\underline{H}_2$NH-geranyl), 57.7 (2-adamantyl), 122.7 (2-geranyl), 124.4 (6-geranyl), 131.9 (7-geranyl), 138.5 (3-geranyl); HRMS (ESI-TOF (+)) *m/z* [M + H]$^+$ calculated for [C$_{24}$H$_{43}$N$_2$]$^+$ 359.3421, found 359.342; Purity of the product determined by HPLC-MS: 95.9%.

2-((3,7-Dimethylocta-2,6-dien-1-yl)amino)-N-(2-propyladamantan-2-yl)acetamide, **7d**
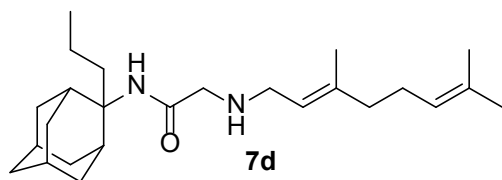

Bromoacetamide **6d** (850 mg, 2.70 mmol) in dry THF (15 mL) was added dropwise at 0 °C to a stirred solution of geranylamine (**2**) (413 mg, 2.70 mmol) and triethylamine (273 mg, 2.70 mmol) in dry THF (25 mL). The stirring continued for 48 h at room temperature. Then the aqueous phase was extracted twice with dichloromethane, the combined organic extracts were evaporated in vacuo and the crude

product was purified through column chromatography using a. ether:n-hexane (1:1), b. $CHCl_3$:MeOH (9:1), as eluents. Acetamide **7d** was obtained as a pale yellow oil; yield 750 mg (72%); ^{1}H-NMR (CDCl$_3$, 400 MHz) δ (ppm) 0.89 (t, J = 7.4 Hz, 3H, 2-adamantyl CH$_2$CH$_2$C$\underline{H}_3$), 1.12-1.25 (m, 2H, 2-adamantyl CH$_2$C$\underline{H}_2$CH$_3$), 1.58-1.71 (m, 21H, 1,3,4eq,8eq,9eq,10eq-adamantyl, 8-geranyl, 3,7-geranyl CH$_3$, 2-adamantyl C$\underline{H}_2$CH$_2$CH$_3$), 1.81 (s, 2H, 6-adamantyl), 1.96-2.05 (m, 8H, 5,7,8ax,10ax-adamantyl, 4,5-geranyl), 2.24 (d, J = 12 Hz, 2H, 4ax,9ax-adamantyl) 3.19 (d, J = 7.4 Hz, 2H, 1-geranyl) 3.30-3.31 (m, 2H, COC$\underline{H}_2$NH), 5.07 (m, 1H, 6-geranyl), 5.24 (m, 1H, 2-geranyl); ^{13}C-NMR (CDCl$_3$, 100MHz) δ (ppm) 14.9 (2-adamantyl CH$_2$CH$_2$C$\underline{H}_3$), 15.0 (2-adamantyl CH$_2$C$\underline{H}_2$CH$_3$), 16.4 (3-geranyl CH$_3$), 18.0 (8-geranyl), 26.0 (7-geranyl CH$_3$), 26.8 (5-geranyl), 27.6 (5,7-adamantyl), 33.3 (4,9-adamantyl), 33.5 (8,10-adamantyl), 33.7 (1,3-adamantyl), 33.9 (2-adamantyl $\underline{C}$H$_2$CH$_2$CH$_3$), 35.4 (6-adamantyl), 39.0 (4-geranyl), 40.0 (1-geranyl), 47.5 (CO$\underline{C}$H$_2$NH), 52.0 (2-adamantyl), 119.7 (2-geranyl), 124.2 (6-geranyl), 132.1 (7-geranyl), 140.1 (3-geranyl), 168.7 (C=O); HRMS (ESI-TOF (+)) m/z [M + H]$^+$ calculated for [C$_{25}$H$_{43}$N$_2$O]$^+$ 387.337, found 387.337.

N-(3,7-dimethylocta-2,6-dien-1-yl)-N´-(2-propyladamantan-2-yl)ethane-1,2-diamine, **8d**
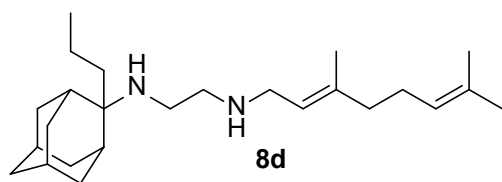
Acetamide **7d** (1.22 g, 3.16 mmol) in dry dichloromethane (14 mL) was stirred at 0-5 °C for 15 min under argon atmosphere. Recently distilled trimethylsilyl chloride (412 µL, 3.79 mmol) was then added at the same temperature and the mixture was stirred for another 15 min. A suspension of LiAlH$_4$ (168 mg, 4.42 mmol) in a small quantity of THF was added at -10-0°C and the stirring continued for 2.5 h at the same temperature. The mixture was then treated with NaOH 10%, the resulting inorganic precipitate was filtered off, the organic phase was separated and the aqueous phase was extracted twice with dichloromethane. The combined organic extracts were evaporated in vacuo and the crude product was dissolved in dichloromethane and washed with brine. After the evaporation of the solvent, the mixture was purified through column chromatography using a. CHCl$_3$:MeOH (9:1), b. CHCl$_3$:MeOH:NH$_3$ (88:10:2), as system solvents to afford diamine **8d** as a pale yellow oil; yield 390 mg (33%); ^{1}H-NMR (CDCl$_3$, 400 MHz) δ (ppm) 0.90 (t, J = 7.4 Hz, 3H, 2-adamantyl CH$_2$CH$_2$C$\underline{H}_3$), 1.15-1.25 (m, 2H, 2-adamantyl CH$_2$C$\underline{H}_2$CH$_3$), 1.45 (d, J = 12 Hz, 2H, 4eq,9eq-adamantyl), 1.55-1.72 (m, 17H, 1,3,6,8eq,10eq-adamantyl, 8-geranyl, 3,7-geranyl CH$_3$, 2-adamantyl C$\underline{H}_2$CH$_2$CH$_3$), 1.79 (d, J = 12 Hz,

2H, 5,7-adamantyl), 1.92 (d, J = 11.4 Hz, 2H, 8ax,10ax-adamantyl), 1.90-2.02 (m, 2H, 5-geranyl), 2.06-2.11 (m, 2H, 4-geranyl), 2.15 (d, J = 12.5 Hz, 4ax,9ax-adamantyl), 2.52 (t, J = 6Hz, 2H, NHC$\underline{H_2}$CH$_2$NH-geranyl), 2.69 (t, J = 6 Hz, 2H, NHCH$_2$C$\underline{H_2}$NH-geranyl), 3.23 (d, J = 7.0 Hz, 2H, 1-geranyl), 5.08 (t, J = 7 Hz, 1H, 6-geranyl), 5.25 (t, J = 7 Hz, 1H, 2-geranyl); ^{13}C NMR (CDCl$_3$, 100MHz) δ (ppm) 15.2 (2-adamantyl CH$_2$CH$_2$$\underline{C}H_3$), 15.3 (2-adamantyl CH$_2$$\underline{C}H_2CH_3$), 16.6 (3-geranyl CH$_3$), 18.0 (8-geranyl), 26.0 (7-geranyl CH$_3$), 26.9 (5-geranyl C), 28.1 (5-adamantyl), 28.3 (7-adamantyl), 33.0 (4,9-adamantyl), 34.0 (8,10-adamantyl), 34.4 (1,3-adamantyl), 34.6 (2-adamantyl $\underline{C}$H$_2$CH$_2$CH$_3$), 39.5 (6-adamantyl), 39.7 (4-geranyl), 40.0 (1-geranyl), 47.5 (NH$\underline{C}$H$_2$CH$_2$NH-geranyl), 50.5 (NHCH$_2$$\underline{C}H_2$NH-geranyl), 57.5 (2-adamantyl), 123.3 (2-geranyl), 124.5 (6-geranyl), 131.8 (7-geranyl), 137.9 (3-geranyl); HRMS (ESI-TOF (+)) m/z [M + H]$^+$ calculated for [C$_{25}$H$_{45}$N$_2$]$^+$ 373.3577, found 373.3575; Purity of the product determined by HPLC-MS: 100.0%.

N-(3,7-dimethylocta-2,6-dien-1-yl)-2-((2-propyladamantan-2-yl)amino)acetamide, **14d**

14d

Acetamide **13** (184 mg, 0.67 mmol) in dry THF (6 mL) was added dropwise at 0 °C to a stirred solution of 2-propyl-2-adamantanamine (**5d**) (130 mg, 0.67 mmol) and triethylamine (68 mg, 0.67 mmol) in dry THF (8 mL). The stirring continued for 48 h at room temperature. Then the aqueous phase was extracted twice with dichloromethane, the combined organic extracts were evaporated in vacuo and the crude product was purified through column chromatography using a. ether:n-hexane (1:1), b. CHCl$_3$:MeOH (9:1), as eluents. Acetamide **14d** was obtained as a pale yellow oil; yield 90 mg (35%); ^{1}H-NMR (CDCl$_3$, 400 MHz) δ (ppm) 0.90 (t, J = 7.4 Hz, 3H, 2-adamantyl CH$_2$CH$_2$C$\underline{H_3}$), 1.14-1.20 (m, 2H, 2-adamantyl CH$_2$C$\underline{H_2}$CH$_3$), 1.51-1.68 (m, 21H, 1,3,4,6,8eq,9,10eq-adamantyl, 8-geranyl, 3,7-geranyl CH$_3$, 2-adamantyl C$\underline{H_2}$CH$_2$CH$_3$), 1.83 (s, 2H, 5,7-adamantyl), 1.90-1.93 (m, 2H, 4ax,9ax-adamantyl), 2.01-2.09 (m, 4H, 4,5-geranyl), 3.12 (s, 2H, NHC$\underline{H_2}$CO), 3.87 (t, J = 6 Hz, 2H, 1-geranyl), 5.08 (t, J = 7 Hz, 1H, 6-geranyl), 5.20 (t, J = 7 Hz, 1H, 2-geranyl); ^{13}C-NMR (CDCl$_3$, 100MHz) δ (ppm) 15.0 (2-adamantyl CH$_2$CH$_2$$\underline{C}H_3$), 15.5 (2-adamantyl CH$_2$$\underline{C}H_2CH_3$), 16.6 (3-geranyl CH$_3$), 18.0 (8-geranyl), 26.0 (7-geranyl CH$_3$), 26.8 (5-geranyl), 28.0 (5,7-adamantyl), 33.2 (4,9-adamantyl), 33.8 (8,10-adamantyl), 34.4 (1,3-adamantyl), 35.2 (2-adamantyl $\underline{C}$H$_2$CH$_2$CH$_3$), 37.2 (6-adamantyl), 39.3 (4-geranyl), 39.8 (1-geranyl), 44.2 (NH$\underline{C}$H$_2$CO), 120.4 (2-geranyl), 124.2 (6-geranyl), 132.1 (7-geranyl), 140.1 (3-geranyl),

168.8 (C=O); HRMS (ESI-TOF (+)) *m/z* [M + H]⁺ calculated for $[C_{25}H_{43}N_2O]^+$ 387.337, found 387.3369; Purity of the product determined by HPLC-MS: 98.3%.
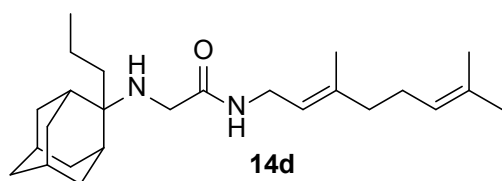
2-((3,7-Dimethylocta-2,6-dien-1-yl)amino)-N-(2-butyladamantan-2-yl)acetamide, **7e**

Bromoacetamide **6e** (190 mg, 0.58 mmol) in dry THF (4 mL) was added dropwise at 0 °C to a stirred solution of geranylamine (**2**) (89 mg, 0.58 mmol) and triethylamine (58 mg, 0.58 mmol) in dry THF (5 mL). The stirring continued for 72 h at room temperature. Then the aqueous phase was extracted twice with dichloromethane, the combined organic extracts were evaporated in vacuo and the crude product was purified through column chromatography using a. ether:n-hexane (1:1), b. CHCl₃:MeOH (9:1), as eluents. Acetamide **7e** was obtained as a pale yellow oil; yield 160 mg (69%); ¹H-NMR (CDCl₃, 400 MHz) *δ* (ppm) 0.73-0.77 (m, 3H, 2-adamantyl (CH₂)₃CH₃), 1.08-1.34 (m, 4H, 2-adamantyl CH₂(CH₂)₂CH₃), 1.60 (s, 3H, 8-geranyl), 1.63 (s, 3H, 7-geranyl CH₃), 1.68 (s, 3H, 3-geranyl CH₃), 1.59-1.71 (m, 6H, 1,3,4eq,8eq,9eq,10eq-adamantyl), 1.82 (s, 2H, 6-adamantyl), 1.89-2.08 (m, 10H, 5,7,8ax,10ax-adamantyl, 2-adamantyl CH₂(CH₂)₂CH₃, 4,5-geranyl), 2.24 (d, *J* = 12.5 Hz, 2H, 4ax,9ax-adamantyl), 3.20 (d, *J* = 7.4 Hz, 2H, 1-geranyl), 3.30 (s, 2H, COCH₂NH), 5.07 (t, *J* = 7.4 Hz, 1H, 6-geranyl), 5.24 (t, *J* = 7.4 Hz, 1H, 2-geranyl). Fumarate salt; ¹³C-NMR (MeOD, 100MHz,) *δ* (ppm) 14.5 (2-adamantyl (CH₂)₃CH₃), 15.6 (3-geranyl CH₃), 16.8 (8-geranyl), 18.0 (7-geranyl CH₃), 23.5 (4,9-adamantyl), 25.4 (5-geranyl), 26.0 (2-adamantyl (CH₂)₂CH₂CH₃), 26.8 (2-adamantyl CH₂CH₂CH₂CH₃), 27.6 (5,7-adamantyl), 32.7 (2-adamantyl CH₂(CH₂)₂CH₃), 33.3 (8,10-adamantyl), 33.7 (1,3-adamantyl), 39.0 (6-adamantyl), 40.0 (4-geranyl), 47.3 (1-geranyl), 60.8 (COCH₂NH), 66.2 (2-adamantyl), 119.8 (2-geranyl), 124.1 (6-geranyl), 132.2 (3,7-geranyl), 168.7 (C=O); HRMS (ESI-TOF (+)) *m/z* [M + H]⁺ calculated for $[C_{26}H_{45}N_2O]^+$ 401.3526, found 401.3527; Purity of the product determined by HPLC-MS: 98.6%.

N-(3,7-dimethylocta-2,6-dien-1-yl)-N´-(2-butyladamantan-2-yl)ethane-1,2-diamine, **8e**

8e

Acetamide **7e** (160 mg, 0.40 mmol) in dry dichloromethane (2 mL) was stirred at 0-5 °C for 15 min under argon atmosphere. Recently distilled trimethylsilyl chloride (52 μL, 0.48 mmol) was then added at the same temperature and the mixture was stirred for another 15 min. A suspension of LiAlH$_4$ (21 mg, 0.56 mmol) in a small quantity of THF was added at -10-0°C and the stirring continued for 2.5 h at the same temperature. The mixture was then treated with NaOH 10%, the resulting inorganic precipitate was filtered off, the organic phase was separated and the aqueous phase was extracted twice with dichloromethane. The combined organic extracts were evaporated in vacuo and the crude product was dissolved in dichloromethane and washed with brine. After the evaporation of the solvent, the crude product was purified through column chromatography using ether:n-hexane (1:1) and a gradient of CHCl$_3$:MeOH (25:1, 20:1), as system solvents to afford diamine **8e** as a pale yellow oil; yield 20 mg (13%). Fumarate salt; ^{1}H-NMR (MeOD, 400 MHz) δ (ppm) 0.91 (t, J = 7Hz, 3H, 2-adamantyl (CH$_2$)$_3$C$\underline{H}$$_3$), 1.12-1.33 (m, 4H, 2-adamantyl CH$_2$(C$\underline{H}$$_2$)$_2CH_3$), 1.49 (d, J = 12Hz, 2H, 4eq,9eq-adamantyl), 1.59 (s, 3H, 8-geranyl), 1.64 (s, 3H, 7-geranyl CH$_3$), 1.67 (s, 3H, 3-geranyl CH$_3$), 1.59-1.69 (m, 8H, 1,3,6,8eq,10eq-adamantyl, 2-adamantyl-C$\underline{H}$$_2$(CH$_2$)$_2CH_3$), 1.81 (s, 2H, 5,7-adamantyl), 1.92 (d, J = 12Hz, 2H, 8ax,10ax-adamantyl), 1.99-2.11 (m, 4H, 4,5-geranyl), 2.16 (d, J =12Hz, 2H, 4ax,9ax-adamantyl), 2.59 (t, J = 6Hz, 2H, NHC$\underline{H}$$_2CH_2$NH-geranyl), 2.79 (t, J = 6 Hz, 2H, NHCH$_2$C$\underline{H}$$_2$NH-geranyl), 3.29 (d, J = 7.0 Hz, 2H, 1-geranyl), 5.08 (t, J = 7 Hz, 1H, 6-geranyl), 5.26 (t, J = 7 Hz, 1H, 2-geranyl); ^{13}C NMR (MeOD, 100MHz) δ (ppm) 15.4 (2-adamantyl (CH$_2$)$_3$C$\underline{H}$$_3$), 17.5 (3-geranyl CH$_3$), 18.7 (8-geranyl), 19.7 (7-geranyl CH$_3$), 23.4 (5-geranyl), 25.2 (4-adamantyl), 25.7 (9-adamantyl), 26.7 (2-adamantyl (CH$_2$)$_2$C$\underline{H}$$_2CH_3$), 28.1 (2-adamantyl CH$_2C\underline{H}$$_2CH_2CH_3$), 29.8 (5,7-adamantyl), 33.1 (2-adamantyl C$\underline{H}$$_2$(CH$_2$)$_2CH_3$), 34.1 (8-adamantyl), 35.4 (10-adamantyl), 35.7 (1,3-adamantyl), 38.9 (6-adamantyl), 40.8 (4-geranyl), 41.6 (1-geranyl), 47.3 (NHC$\underline{H}$$_2CH_2$NH-geranyl), 48.2 (NHCH$_2C\underline{H}$$_2$NH-geranyl), 62.1 (2-adamantyl), 117.2 (2-geranyl), 125.6 (6-geranyl), 136.7 (3,7-geranyl); HRMS (ESI-TOF (+)) m/z [M + H]$^+$ calculated for [C$_{26}$H$_{47}$N$_2$]$^+$ 387.3734, found 387.3737; Purity of the product determined by HPLC-MS: 98.2%.

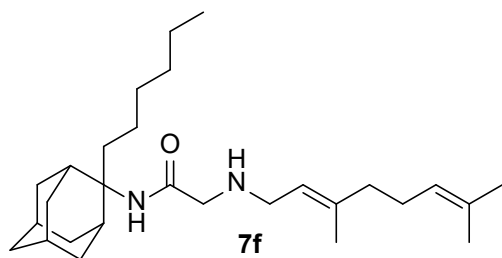*2-((3,7-Dimethylocta-2,6-dien-1-yl)amino)-N-(2-hexyladamantan-2-yl)acetamide,* **7f**

7f

Bromoacetamide **6f** (70 mg, 0.20 mmol) in dry THF (1.5 mL) was added dropwise at 0 °C to a stirred solution of geranylamine (**2**) (31 mg, 0.20 mmol) and triethylamine (20 mg, 0.20 mmol) in dry THF (2 mL). The stirring continued for 72 h at room temperature. Then the aqueous phase was extracted twice with dichloromethane, the combined organic extracts were evaporated in vacuo and the crude product was purified through column chromatography using a. ether:n-hexane (1:1), b. $CHCl_3$:MeOH (9:1), as eluents. Acetamide **7f** was obtained as a yellow oil; yield 50 mg (60%); ^{1}H-NMR (CDCl$_3$, 400 MHz) δ (ppm) 0.88 (t, J = 7Hz, 3H, 2-adamantyl (CH$_2$)$_5$C$\underline{H}_3$), 1.11-1.33 (m, 8H, 2-adamantyl CH$_2$(C$\underline{H}_2$)$_4$CH$_3$), 1.51-1.68 (m, 19H, 1,3,4eq,6,8eq,9eq,10eq-adamantyl, 3-geranyl CH$_3$, 7-geranyl CH$_3$, 8-H, 2-adamantyl C$\underline{H}_2$(CH$_2$)$_4$CH$_3$), 1.82-1.83 (m, 2H, 5,7-adamantyl), 1.91 (d, J = 8.5 Hz, 2H, 8ax,10ax-adamantyl), 2.01-2.10 (m, 6H, 4ax,9ax-adamantyl, 4,5-geranyl), 3.11 (s, 2H, COC$\underline{H}_2$NH), 3.88 (t, J = 4 Hz, 2H, 1-geranyl), 5.08 (t, J = 7.4 Hz, 1H, 6-geranyl), 5.21 (t, J = 7.4 Hz, 1H, 2-geranyl); ^{13}C-NMR (CDCl$_3$, 100MHz) δ (ppm) 15.6 (2-adamantyl (CH$_2$)$_5$$\underline{C}H_3$), 16.6 (3-geranyl CH$_3$), 18.0 (8-geranyl), 22.2 (2-adamantyl (CH$_2$)$_4$$\underline{C}H_2CH_3$), 23.0 (2-adamantyl (CH$_2$)$_3$$\underline{C}H_2CH_2CH_3$), 26.0 (7-geranyl CH$_3$), 26.8 (5-geranyl), 28.0 (5,7-adamantyl), 30.3 (2-adamantyl CH$_2$)$_2$$\underline{C}H_2$(CH$_2$)$_2CH_3$), 32.4 (2-adamantyl CH$_2$$\underline{C}H_2$(CH$_2$)$_3CH_3$), 32.7 (2-adamantyl $\underline{C}$H$_2$(CH$_2$)$_4$CH$_3$), 33.3 (4,9-adamantyl), 33.9 (8,10-adamantyl), 34.4 (1,3-adamantyl), 37.2 (6-adamantyl), 39.3 (4-geranyl), 39.8 (1-geranyl), 58.0 (CO$\underline{C}$H$_2$NH), 66.2 (2-adamantyl), 120.5 (2-geranyl), 124.2 (6-geranyl), 132.1 (7-geranyl), 140.1 (3-geranyl), 172.8 (C=O).

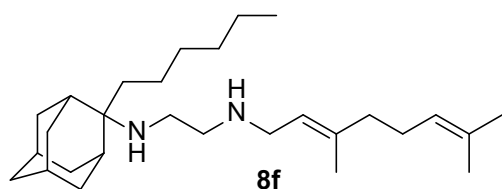*N-(3,7-dimethylocta-2,6-dien-1-yl)-N´-(2-hexyladamantan-2-yl)ethane-1,2-diamine,* **8f**

8f

Acetamide **7f** (50 mg, 0.12 mmol) in dry dichloromethane (1 mL) was stirred at 0-5 °C for 15 min under argon atmosphere. Recently distilled trimethylsilyl chloride (15 μL, 0.14 mmol) was then added at the same temperature and the mixture was stirred for another 15 min. A suspension of LiAlH$_4$ (7

mg, 0.17 mmol) in a small quantity of THF was added at -10-0 $^\circ$C and the stirring continued for 2.5 h at the same temperature. The mixture was then treated with NaOH 10%, the resulting inorganic precipitate was filtered off, the organic phase was separated and the aqueous phase was extracted twice with dichloromethane. The combined organic extracts were evaporated in vacuo and the crude was dissolved in dichloromethane and washed with brine. After the evaporation of the solvent, the crude product was purified through column chromatography using ether:n-hexane (1:1) and CHCl$_3$:MeOH (30:1), as system solvents to afford diamine **8f** as a yellow oil; yield 20 mg (40%); ^{1}H-NMR (CDCl$_3$, 400 MHz) δ (ppm) 0.87 (t, J = 7Hz, 3H, 2-adamantyl (CH$_2$)$_5$C$\underline{H}_3$), 1.18-1.27 (m, 8H, 2-adamantyl CH$_2$(C$\underline{H}_2$)$_4$CH$_3$), 1.49 (d, J = 12Hz, 2H, 4eq,9eq-adamantyl), 1.59 (s, 3H, 8-geranyl), 1.64 (s, 3H, 7-geranyl CH$_3$), 1.66 (s, 3H, 3-geranyl CH$_3$), 1.59-1.69 (m, 8H, 1,3,6,8eq,10eq-adamantyl, 2-adamantyl C$\underline{H}_2$(CH$_2$)$_4$CH$_3$), 1.81 (s, 2H, 5,7-adamantyl), 1.91 (d, J = 8.5 Hz, 2H, 8ax,10ax-adamantyl), 1.99-2.10 (m, 4H, 4,5-geranyl), 2.16 (d, J = 8.5 Hz, 2H, 4ax,9ax-adamantyl), 2.58 (t, J = 6Hz, 2H, NHC$\underline{H}_2$CH$_2$NH-geranyl), 2.78 (t, J = 6 Hz, 2H, NHCH$_2$C$\underline{H}_2$NH-geranyl), 3.29 (d, J = 7.0 Hz, 2H, 1-geranyl), 5.07 (t, J = 7 Hz, 1H, 6-geranyl), 5.25 (t, J = 7 Hz, 1H, 2-geranyl); ^{13}C NMR (CDCl$_3$, 100MHz) δ (ppm) 14.4 (2-adamantyl (CH$_2$)$_5$$\underline{C}H_3$), 16.7 (3-geranyl CH$_3$), 18.0 (8-geranyl), 22.0 (2-adamantyl (CH$_2$)$_4$$\underline{C}H_2CH_3$), 23.1 (2-adamantyl (CH$_2$)$_3$$\underline{C}H_2CH_2CH_3$), 26.0 (7-geranyl CH$_3$), 26.8 (5-geranyl), 27.9 (5,7-adamantyl), 30.4 (2-adamantyl CH$_2$)$_2$$\underline{C}H_2$(CH$_2$)$_2CH_3$, 32.0 (2-adamantyl CH$_2$$\underline{C}H_2$(CH$_2$)$_3CH_3$), 32.3 (2-adamantyl $\underline{C}$H$_2$(CH$_2$)$_4$CH$_3$), 32.9 (4,9-adamantyl), 33.9 (8,10-adamantyl), 34.2 (1,3-adamantyl), 39.1 (6-adamantyl), 39.3 (4-geranyl), 40.0 (1-geranyl), 46.9 (NH$\underline{C}$H$_2$CH$_2$NH-geranyl), 49.2 (NHCH$_2$$\underline{C}H_2$NH-geranyl), 66.2 (2-adamantyl), 121.9 (2-geranyl), 124.3 (6-geranyl), 131.9 (7-geranyl), 139.2 (3-geranyl); HRMS (ESI-TOF (+)) m/z [M + H]$^+$ calculated for [C$_{28}$H$_{51}$N$_2$]$^+$ 415.4047, found 415.404; Purity of the product determined by HPLC-MS: 100.0%.

2-((3,7-Dimethylocta-2,6-dien-1-yl)amino)-N-(2-benzyladamantan-2-yl)acetamide, **7g**
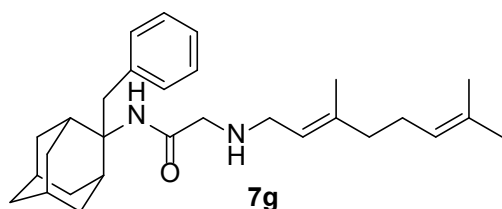
Bromoacetamide **6g** (530 mg, 1.46 mmol) in dry THF (8 mL) was added dropwise at 0 $^\circ$C to a stirred solution of geranylamine (**2**) (223 mg, 1.46 mmol) and triethylamine (147 mg, 1.46 mmol) in dry THF (12.5 mL). The stirring continued for 48 h at room temperature. Then the aqueous phase was

extracted twice with dichloromethane, the combined organic extracts were evaporated in vacuo and the crude product was purified through column chromatography using a. ether:n-hexane (1:1), b. CHCl$_3$:MeOH (9:1), as eluents. Acetamide **7g** was obtained as a pale yellow oil; yield 560 mg (88%); ^{1}H-NMR (CDCl$_3$, 400 MHz) δ (ppm) 1.57 (s, 3H, 8-geranyl), 1.59 (s, 3H, 7-geranyl CH$_3$), 1.67 (s, H, 3-geranyl CH$_3$), 1.57-1.84 (m, 9H, 1,3,4eq,5,6eq,7,8eq,9eq,10eq-adamantyl), 1.90 (s, 1H, 6ax-adamantyl), 1.98-2.08 (m, 4H, 4,5-geranyl), 2.24-2.30 (m, 4H, 4ax,8ax,9ax,10ax-adamantyl), 3.14 (d, J = 7.4 Hz, 2H, 1-geranyl), 3.25 (s, 2H, COC<u>H</u>$_2$NH), 3.38 (s, 2H, benzyl), 5.07 (t, J = 7.4 Hz, 1H, 6-geranyl), 5.26 (t, J = 7.4 Hz, 1H, 2-geranyl), 7.06-7.14 (m, 2H, phenyl), 7.16-7.19 (m, 1H, phenyl), 7.22-7.25 (m, 2H, phenyl); ^{13}C-NMR (CDCl$_3$, 100MHz) δ (ppm) 16.8 (3-geranyl CH$_3$), 18.0 (8-geranyl), 26.0 (7-geranyl CH$_3$), 26.7 (5-geranyl), 27.3 (5-adamantyl), 27.8 (7-adamantyl), 33.5 (4,8,9,10-adamantyl), 33.6 (1,3-adamantyl), 38.1 (benzyl), 38.9 (6-adamantyl), 39.9 (4-geranyl), 47.1 (1-geranyl), 56.7 (CO<u>C</u>H$_2$NH), 62.0 (2-adamantyl), 123.9 (6-geranyl), 126.5 (phenyl), 128.3 (phenyl), 130.6 (phenyl), 138.5 (quaternary-phenyl), 163.6 (C=O); HRMS (ESI-TOF (+)) m/z [M + H]$^+$ calculated for [C$_{29}$H$_{43}$N$_2$O]$^+$ 435.337, found 435.3371; Purity of the product determined by HPLC-MS: 97.8%.

N-(3,7-dimethylocta-2,6-dien-1-yl)-N´-(2-benzyladamantan-2-yl)ethane-1,2-diamine, **8g**
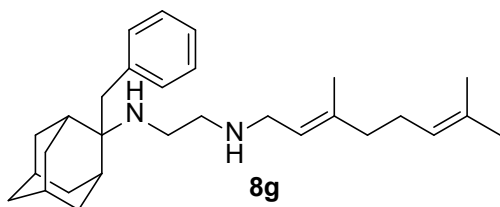
Acetamide **7g** (560 mg, 1.29 mmol) in dry dichloromethane (5 mL) was stirred at 0-5 °C for 15 min under argon atmosphere. Recently distilled trimethylsilyl chloride (168 μL, 1.55 mmol) was then added at the same temperature and the mixture was stirred for another 15 min. A suspension of LiAlH$_4$ (69 mg, 1.81 mmol) in a small quantity of THF was added at -10-0°C and the stirring continued for 2.5 h at the same temperature. The mixture was then treated with NaOH 10%, the resulting inorganic precipitate was filtered off, the organic phase was separated and the aqueous phase was extracted twice with dichloromethane. The combined organic extracts were evaporated in vacuo and the crude product was dissolved in dichloromethane and washed with brine. After the evaporation of the solvent, the crude product was purified through column chromatography using ether:n-hexane (1:1) and CHCl$_3$:MeOH (9:1), as system solvents to afford diamine **8f** as a pale yellow oil; yield 141 mg (26%); ^{1}H-NMR (CDCl$_3$, 400 MHz) δ (ppm) 1.45 (d, J = 12Hz, 2H, 4eq,9eq-adamantyl), 1.59 (s, 3H, 8-

geranyl), 1.63 (s, 3H, 7-geranyl CH$_3$), 1.67 (s, 3H, 3-geranyl CH$_3$), 1.59-1.75 (m, 6H, 1,3,5,7,8eq,10eq-adamantyl), 1.81 (s, 1H, 6eq-adamantyl), 1.95 (s, 1H, 6ax-adamantyl), 1.99-2.10 (m, 4H, 4,5-geranyl), 2.18-2.23 (m, 4H, 4ax,8ax,9ax,10ax-adamantyl), 2.75 (t, J = 6Hz, 2H, NHC$\underline{H}_2$CH$_2$NH-geranyl), 2.84 (t, J = 6 Hz, 2H, NHCH$_2$C$\underline{H}_2$NH-geranyl), 2.99 (s, 2H, benzyl), 3.32 (d, J = 7 Hz, 2H, 1-geranyl), 5.07 (t, J = 7 Hz, 1H, 6-geranyl), 5.26 (t, J = 7 Hz, 1H, 2-geranyl), 7.16-7.30 (m, 5H, phenyl); ^{13}C NMR (CDCl$_3$, 100MHz) δ (ppm) 16.8 (3-geranyl CH$_3$), 18.0 (8-geranyl), 26.0 (7-geranyl CH$_3$), 26.8 (5-geranyl), 27.8 (5-adamantyl), 28.3 (7-adamantyl), 33.1 (4,9-adamantyl), 34.0 (8,10-adamantyl), 34.4 (1,3-adamantyl), 37.3 (benzyl), 38.8 (NHC$\underline{H}_2$CH$_2$NH-geranyl), 39.3 (6-adamantyl), 39.9 (4-geranyl), 46.9 (1-geranyl), 49.3 (NHCH$_2$C$\underline{H}_2$NH-geranyl), 59.0 (2-adamantyl), 124.2 (6-geranyl), 126.4 (phenyl), 128.5 (phenyl), 130.5 (phenyl), 132.0 (7-geranyl), 138.7 (quaternary-phenyl); HRMS (ESI-TOF (+)) m/z [M + H]$^+$ calculated for [C$_{29}$H$_{45}$N$_2$]$^+$ 421.3577, found 421.3571; Purity of the product determined by HPLC-MS: 98.6%.

2-((3,7-Dimethylocta-2,6-dien-1-yl)amino)-N-(2-phenyladamantan-2-yl)acetamide, **7h**

7h
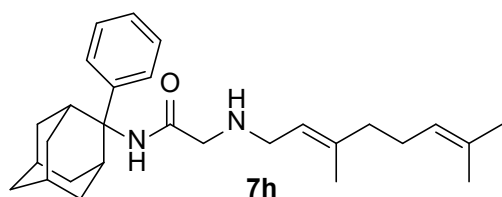
Bromoacetamide **6h** (1.17 g, 3.36 mmol) in dry THF (20 mL) was added dropwise at 0 ℃ to a stirred solution of geranylamine (**2**) (514 mg, 3.36 mmol) and triethylamine (340 mg, 3.36 mmol) in dry THF (30 mL). The stirring continued for 48 h at room temperature. Then the aqueous phase was extracted twice with dichloromethane, the combined organic extracts were evaporated in vacuo and the crude product was purified through column chromatography using a. ether:n-hexane (1:1), b. CHCl$_3$:MeOH (9:1), as eluents. Acetamide **7h** was obtained as a yellow oil; yield 920 mg (35%); ^{1}H-NMR (CDCl$_3$, 400 MHz) δ (ppm) 1.54 (s, 3H, 8-geranyl), 1.60 (s, 3H, 7-geranyl CH$_3$), 1.68 (s, 3H, 3-geranyl CH$_3$), 1.68-2.18 (m, 18H, 1,3,4,5,6,7,8,9,10-adamantyl, 4,5-geranyl), 3.07 (d, J = 7.4 Hz, 2H, 1-geranyl), 3.13 (s, 2H, COC$\underline{H}_2$NH), 5.07 (t, J = 7.4 Hz, 1H, 6-geranyl), 5.14 (t, J = 7.4 Hz, 1H, 2-geranyl), 7.17-7.33 (m, 3H, phenyl), 7.58-7.59 (m, 2H, phenyl); ^{13}C-NMR (CDCl$_3$, 100MHz) δ (ppm) 16.6 (3-geranyl CH$_3$), 18.0 (8-geranyl), 26.0 (7-geranyl CH$_3$), 26.8 (5-geranyl), 27.0 (5-adamantyl), 27.8 (7-adamantyl), 32.8 (4,9-adamantyl), 33.7 (1,3,8,10-adamantyl), 38.2 (6-adamantyl), 39.9 (4-geranyl), 47.4 (1-geranyl), 52.6 (COC$\underline{H}_2$NH), 61.0 (2-adamantyl), 122.1 (2-geranyl), 124.3 (6-geranyl), 126.7 (phenyl), 128.3 (phenyl),

132.0 (7-geranyl), 139.3 (quaternary-phenyl), 143.5 (3-geranyl), 169.8 (C=O); HRMS (ESI-TOF (+)) *m/z* [M + H]$^+$ calculated for [C$_{28}$H$_{41}$N$_2$O]$^+$ 421.3213, found 421.3214; Purity of the product determined by HPLC-MS: 97.8%.

N-(3,7-dimethylocta-2,6-dien-1-yl)-N´-(2-phenyl-adamantan-2-yl)ethane-1,2-diamine, **8h**
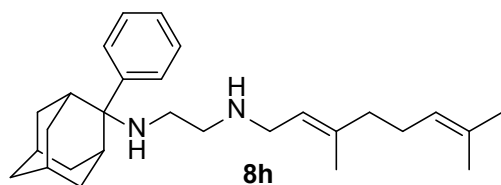
Acetamide **7h** (800 mg, 1.90 mmol) in dry dichloromethane (10 mL) was stirred at 0-5 ℃ for 15 min under argon atmosphere. Recently distilled trimethylsilyl chloride (247 µL, 2.28 mmol) was then added at the same temperature and the mixture was stirred for another 15 min. A suspension of LiAlH$_4$ (101 mg, 2.66 mmol) in a small quantity of THF was added at -10-0℃ and the stirring continued for 2.5 h at the same temperature. The mixture was then treated with NaOH 10%, the resulting inorganic precipitate was filtered off, the organic phase was separated and the aqueous phase was extracted twice with dichloromethane. The combined organic extracts were evaporated in vacuo and the crude product was dissolved in dichloromethane and washed with brine. After the evaporation of the solvent, the crude product was purified through column chromatography using ether:n-hexane (1:1) and CHCl$_3$:MeOH (9:1), as system solvents to afford the diamine **8h** as a pale yellow oil; yield 290 mg (36%); ^{1}H-NMR (CDCl$_3$, 400 MHz) *δ* (ppm) 1.56 (s, 3H, 8-geranyl), 1.59 (s, 3H, 7-geranyl CH$_3$), 1.67 (s, 3H, 3-geranyl CH$_3$), 1.67-1.75 (m, 9H, 1,3,4eq,5,6eq,7,8eq,9eq,10eq-adamantyl), 1.89 (s, 1H, 6ax-adamantyl), 1.98-2.09 (m, 4H, 4,5-geranyl), 2.40 (d, *J* = 12.3Hz, 2H, 8ax,10ax-adamantyl), 2.23 (t, *J* = 6Hz, 2H, NHC**H$_2$**CH$_2$NH-geranyl), 2.48-2.51 (m, 4H, 4ax,9ax-adamantyl, NHCH$_2$C**H$_2$**NH-geranyl), 3.05 (d, *J* = 7.0 Hz, 2H, 1-geranyl), 5.07 (t, *J* = 7 Hz, 1H, 6-geranyl), 5.15 (t, *J* = 7 Hz, 1H, 2-geranyl), 7.16-7.20 (m, 1H, phenyl), 7.30-7.37 (m, 4H, phenyl); ^{13}C NMR (CDCl$_3$, 400MHz) *δ* (ppm) 16.6 (3-geranyl CH$_3$), 18.0 (8-geranyl), 26.0 (7-geranyl CH$_3$), 26.8 (5-geranyl C), 27.4 (5-adamantyl), 28.4 (7-adamantyl), 33.0 (4,9-adamantyl), 33.2 (1,3-adamantyl), 34.4 (8,10-adamantyl), 38.5 (6-adamantyl), 39.9 (4-geranyl), 46.7 (1-geranyl), 49.4 (NH**C**H$_2$CH$_2$NH-geranyl), 61.3 (NHCH$_2$**C**H$_2$NH-geranyl), 66.2 (2-adamantyl), 122.2 (2-geranyl), 124.4 (6-geranyl), 126.2 (phenyl), 126.6 (phenyl), 128.4 (phenyl), 131.9 (7-geranyl), 138.8 (quaternary-phenyl), 145.0 (3-geranyl); HRMS (ESI-TOF (+)) *m/z* [M + H]$^+$ calculated for [C$_{28}$H$_{43}$N$_2$]$^+$ 407.3421, found 407.3414; Purity of the product determined by HPLC-MS: 97.0%.
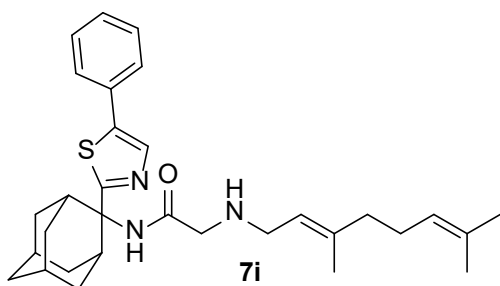
2-((3,7-Dimethylocta-2,6-dien-1-yl)amino)-N-(2-(5-phenylthiazol-2-yl)adamantan-2-yl)acetamide, **7i**

Bromoacetamide **6i** (414 mg, 0.96 mmol) in dry THF (6 mL) was added dropwise at 0 °C to a stirred solution of geranylamine (**2**) (147 mg, 0.96 mmol) and triethylamine (97 mg, 0.96 mmol) in dry THF (8.5 mL). The stirring continued for 48 h at room temperature. Then the aqueous phase was extracted twice with dichloromethane, the combined organic extracts were evaporated in vacuo and the crude product was purified through column chromatography using a. ether:n-hexane (1:1), b. CHCl$_3$:MeOH (9:1), as eluents. Acetamide **7i** was obtained as a pale yellow oil; yield 400 mg (83%); ^{1}H-NMR (CDCl$_3$, 400 MHz) δ (ppm) 1.55 (s, 3H, 8-geranyl), 1.59 (s, 3H, 7-geranyl CH$_3$), 1.67 (s, 3H, 3-geranyl CH$_3$), 1.54-1.83 (m, 7H, 4eq,5,6eq,7,8eq,9eq,10eq-adamantyl), 1.86-1.99 (s, 3H, 6ax,8ax,10ax-adamantyl), 2.02-2.17 (m, 6H, 4ax,9ax-adamantyl, 4,5-geranyl), 3.12 (s, 2H, COC$\underline{H}_2$NH), 3.14 (s, 1H, 1,3-adamantyl), 3.16 (m, 2H, 1-geranyl), 5.05 (m, 1H, 6-geranyl), 5.16 (m, 1H, 2-geranyl), 7.27-7.31 (m, 1H, phenyl), 7.36-7.42 (m, 3H, phenyl, thiazoly) 7.85-7.90 (m, 2H, phenyl); ^{13}C-NMR (CDCl$_3$, 100MHz) δ (ppm) 16.6 (3-geranyl CH$_3$), 18.0 (8-geranyl), 26.0 (7-geranyl CH$_3$), 26.8 (5-geranyl), 27.3 (5-adamantyl), 27.4 (7-adamantyl), 33.6 (4,9-adamantyl), 33.9 (8,10-adamantyl), 35.0 (1,3-adamantyl), 38.2 (6-adamantyl), 39.9 (4-geranyl), 47.4 (1-geranyl), 52.5 (CO$\underline{C}$H$_2$NH), 59.0 (2-adamantyl), 113.1 (phenyl), 124.2 (2-geranyl), 126.6 (phenyl), 128.0 (thiazolyl), 128.9 (phenyl), 132.0 (6-geranyl), 135.3 (7-geranyl), 153.7 (3-geranyl), 168.9 (C=O), 170.2 (quaternary-C thiazolyl), 174.6 (quaternary-C thiazolyl); HRMS (ESI-TOF (+)) *m/z* [M + H]$^+$ calculated for [C$_{31}$H$_{42}$N$_3$OS]$^+$ 504.3043, found 504.3054.

N-(3,7-dimethylocta-2,6-dien-1-yl)-N´-(2-(5-phenylthiazol-2-yl)adamantan-2-yl)ethane-1,2-diamine, **8i**

8i
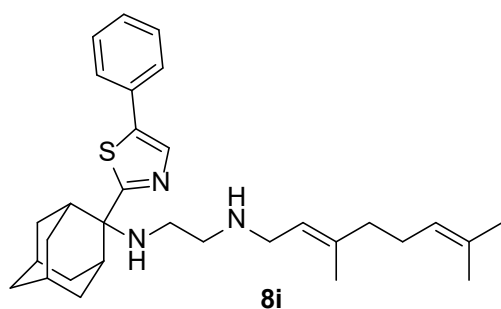
Acetamide **7f** (400 mg, 0.79 mmol) in dry dichloromethane (4 mL) was stirred at 0-5 °C for 15 min under argon atmosphere. Recently distilled trimethylsilyl chloride (103 μL, 0.95 mmol) was then added at the same temperature and the mixture was stirred for another 15 min. A suspension of LiAlH$_4$ (42 mg, 1.11 mmol) in a small quantity of THF was added at -10-0 °C and the stirring continued for 2.5 h at the same temperature. The mixture was then treated with NaOH 10%, the resulting inorganic precipitate was filtered off, the organic phase was separated and the aqueous phase was extracted twice with dichloromethane. The combined organic extracts were evaporated in vacuo and the crude was dissolved in dichloromethane and washed with brine. After the evaporation of the solvent, the crude product was purified through column chromatography using ether:n-hexane (1:1) and CHCl$_3$:MeOH:NH3 (88:10:2), as system solvents to afford diamine **8i** as a pale yellow oil; yield 120 mg (31%); ^{1}H-NMR (CDCl$_3$, 400 MHz) δ (ppm) 1.54 (s, 3H, 8-geranyl), 1.57 (s, 3H, 7-geranyl CH$_3$), 1.65 (s, 3H, 3-geranyl CH$_3$), 1.67-1.79 (m, 7H, 4eq,5,6eq,7,8eq,9eq,10eq-adamantyl), 1.92 (s, 1H, 6ax-adamantyl), 1.99-2.06 (m, 6H, 8ax,10ax-adamantyl, 4,5-geranyl), 2.35-2.38 (d, J = 13.8 Hz, 2H, 4ax,9ax-adamantyl), 2.47 (s, 2H, 1,3-adamantyl), 2.61 (t, J = 5.5Hz, 2H, NHC$\underline{H_2}$CH$_2$NH-geranyl), 2.70 (t, J = 5.5Hz, 2H, NHCH$_2$C$\underline{H_2}$NH-geranyl), 3.29 (d, J = 7.6 Hz, 2H, 1-geranyl), 5.02 (t, J = 7.6 Hz, 1H, 6-geranyl), 5.24 (t, J = 7.6 Hz, 1H, 2-geranyl), 7.28-7.33 (m, 1H, phenyl), 7.38-7.42 (m, 3H, phenyl, thiazolyl), 7.89 (d, J = 6.2 Hz, 2H, phenyl); ^{13}C NMR (CDCl$_3$, 400MHz) δ (ppm) 16.7 (3-geranyl CH$_3$), 18.0 (8-geranyl), 26.0 (7-geranyl CH$_3$), 26.6 (5-geranyl), 27.6 (5-adamantyl), 27.8 (7-adamantyl), 33.0 (4,9-adamantyl), 34.6 (8,10-adamantyl), 35.7 (1,3-adamantyl), 38.5 (6-adamantyl), 39.9 (4-geranyl), 45.1 (1-geranyl), 47.3 (NHC$\underline{H_2}$CH$_2$NH-geranyl), 64.0 (NHCH$_2$C$\underline{H_2}$NH-geranyl), 66.2 (2-adamantyl), 112.5 (phenyl), 124.0 (2-geranyl), 126.6 (phenyl), 128.2 (thiazolyl), 129.0 (phenyl), 132.2 (6-C), 135.1 (7-C), 154.0 (3-C), 178.1 (quaternary-C thiazolyl); HRMS (ESI-TOF (+)) m/z [M + H]$^+$ calculated for [C$_{31}$H$_{44}$N$_3$S]$^+$ 490.3250, found 490.3253. Purity of the product determined by HPLC-MS: 99.3%.

Differential scanning calorimetry. Samples for DSC were prepared by mixing the tested ligands SQ109 (**8a**) and analogs **8b-j, 12** with DMPC or DSPG membranes at 10% w/w concentration. This was

40

achieved by mixing a solution of the ligand's fumarate salt in methanol and a solution of DMPC lipid in chloroform or a solution of DSPC in chloroform/methanol (5:1) and subsequently evaporating the solvent. The films that were formed were utilized for DSC analysis, by weighting approximately 3 mg of each film in a 40 μL aluminum crucible, adding 3 μL of PBS (pH = 7.4) as hydration medium, sealing the crucible, vortexing and allowing it to anneal for a 15 min period, in order to achieve sample equilibration. The DSC thermogram of each sample was obtained by utilizing a DSC822^e Mettler-Toledo calorimeter (Schwerzenbach, Switzerland), calibrated with pure indium (T_m = 156.6 °C). An empty sealed crucible was used as reference. Each analysis included equilibration at 5 °C for 10 min, followed by two heating-cooling cycles in the range between 5-35 °C with a 5 °C/min scanning rate for DMPC samples or between 10-70 °C, with a 2.5 °C/min scanning rate for DSPG samples. The obtained calorimetric data (characteristic transition temperatures T_{onset} and T, transition enthalpy ΔH and width at half peak height of the C_p profiles $\Delta T_{1/2}$) were analyzed with the Mettler-Toledo STAR^e software. The transition enthalpy is expressed as joules per total sample mass and as kilojoules per moles of DMPC and is presented as absolute value in endothermic and exothermic processes (Table 6). LogD values in Table 6 were calculated with ChemAxon software.

Cell growth inhibition assays. Cell growth inhibition assays were performed as previously reported [23, 46, 47] are described in the Supporting Information including representative dose-response curves of SQ109 analogs against the protozoan parasites (Figure S1).

Surface Plasmon Resonance. The MtMmpL3 protein was purified from *M. smegmatis* DmmpL3/pMVGH1-mmpL3tb cells[48] following the previously reported protocol.[10] For the amino coupling of MmpL3tb, CM5 chip surfaces were activated with 0.05 M N-hydroxysuccinimide and 0.2 M N-ethyl-N-(3-diethylaminopropyl)carbodiimide (BIAcore). Purified MmpL3tb was injected over surfaces immediately after activation. The immobilized density of the protein (ligand) was 17,654 response units (RU). For kinetic modeling, we considered only the simplest models that would be compatible with one or two distinct events during both inhibitor binding and dissociation. These four models are (i) simple 1:1 binding model; (ii) heterogeneous ligand (HL), in which different protein populations on-chip surface have different kinetic properties; (iii) two-state reaction or ligand-induced conformational change, wherein conformational change occurs on the same time scale as ligand binding (Figure S2); and (iv) bivalent analyte, where multiple analytes bind independently at nonidentical sites.[10, 49]

The best global fit for compound binding to MmpL3 was obtained using the two-state reaction model. Schematic representations and equations relevant to this model are given below:

(1) $A+B \leftrightarrow A \bullet B \leftrightarrow [A \bullet B*]$,

(2) $\partial(A \bullet B)/\partial t = k_{a1}[A][B] - (k_{d1}[A \bullet B] - k_{d2}[A \bullet B*])$,

(3) $\partial(A \bullet B*)/\partial t = k_{a2}[A \bullet B*] - k_{d2}[A \bullet B*]$,

(4) and $R_t = [A \bullet B] + [A \bullet B*]$.

The equilibrium dissociation constant for this model is:

(5) $K_D = k_{d1}k_{d2}/k_{a1}k_{a2}$,

where [A] is the concentration of analyte; [B] is the ligand binding capacity; [$A \cdot B$] and [$A \cdot B*$] are intermediate and final complexes, respectively; K_{d1}, k_{d2}, k_{a1}, and k_{a2} are microscopic rate constants; and R_t is the total SPR response, which is directly proportional to [$A \cdot B$] + [$A \cdot B*$].

ASSOCIATED CONTENT

Supporting Information.

The Supporting Information is available free of charge at https://pubs.acs.org/doi/XXXX

DSC scans and results for the cooling process of selected SQ109 analogs (one Figure and one Table). A Figure for dose-response curves from biological testing, a Figure with curves from SPR, a Figure with DSC cooling scans, Figures with NMR spectra and HPLC plots. Supplementary information for methods and protocols for synthetic intermediates, biological assays and Supporting Information references.

AUTHOR INFORMATION

Corresponding Authors

Antonios D. Kolocouris− Laboratory of Medicinal Chemistry, Section of Pharmaceutical Chemistry, Department of Pharmacy, National and Kapodistrian University of Athens, Panepistimiopolis-Zografou, Athens 15771, Greece; orcid.org/0000-0001-6110-1903;

Email: ankol@pharm.uoa.gr

Eric Oldfield − Department of Chemistry, University of Illinois at Urbana–Champaign, Urbana, Illinois 61801, USA; orcid.org/0000-0002-0996-7352

Email: eoldfiel@illinois.edu

Authors

Marianna Stampolaki − Laboratory of Medicinal Chemistry, Section of Pharmaceutical Chemistry, Department of Pharmacy, National and Kapodistrian University of Athens, Panepistimiopolis-Zografou, Athens 15771, Greece

Satish R. Malwal − Department of Chemistry, University of Illinois at Urbana–Champaign, Urbana, Illinois 61801, USA; orcid.org/0000-0001-7606-1932

Nadine Alvarez-Cabrera − Center for Discovery and Innovation, Hackensack Meridian Health, Nutley, NJ 07110, USA; orcid.org/0000-0002-9045-5740

Zijun Gao − Department of Chemistry, University of Illinois at Urbana–Champaign, Urbana, Illinois 61801, USA

Mohammad Moniruzzaman − University of Oklahoma, Department of Chemistry and Biochemistry, Stephenson Life Sciences Research Center, 101 Stephenson Parkway, Norman, OK 73019-5251, USA; orcid.org/ 0000-0001-9956-6036

Svitlana O. Babii - University of Oklahoma, Department of Chemistry and Biochemistry, Stephenson Life Sciences Research Center, 101 Stephenson Parkway, Norman, OK 73019-5251, USA; orcid.org/0000-0002-2304-9144

André Rey-Cibati − Instituto de Estudios Avanzados, Caracas, Venezuela Instituto de Biología Experimental, Facultad de Ciencias, Universidad Central de Venezuela (UCV), Caracas, Venezuela; orcid.org/0000-0003-3238-2552

Mariana Valladares-Delgado − Instituto de Estudios Avanzados, Caracas, Venezuela Instituto de Biología Experimental, Facultad de Ciencias, Universidad Central de Venezuela (UCV), Caracas, Venezuela; orcid.org/0000-0001-9917-8543

Nikolaos Naziris − Section of Pharmaceutical Technology, Faculty of Pharmacy, National and Kapodistrian University of Athens, Panepistimiopolis-Zografou, Athens 15771, Greece; orcid.org/0002-8155-3875

Andreea L. Turcu – Laboratori de Química Farmacèutica (Unitat Associada al CSIC), Departament de Farmacologia, Toxicologia i Química Terapèutica, Facultat de Farmàcia i Ciències de l'Alimentació, and Institute of Biomedicine (IBUB), Universitat de Barcelona, Av. Joan XXIII, 27-31, Barcelona, E-08028, Spain; orcid.org/0000-0001-9732-2249

Kyung-Hwa Baek – Host-Parasite Research Laboratory, Institut Pasteur Korea, Seongnam-si, Republic of Korea; orcid.org/0000-0001-6130-281X

Trong-Nhat Phan – Host-Parasite Research Laboratory, Institut Pasteur Korea, Seongnam-si, Republic of Korea; orcid.org/0000-0002-4696-7490

Hyeryon Lee – Host-Parasite Research Laboratory, Institut Pasteur Korea, Seongnam-si, Republic of Korea; orcid.org/0000-0002-8566-7503

Matthéo Alcaraz - Centre National de la Recherche Scientifique UMR 9004, Institut de Recherche en Infectiologie de Montpellier (IRIM), Université de Montpellier, 1919 route de Mende, 34293, Montpellier, France.

Savannah Watson – Department of Biochemistry, Genetics and Microbiology, Institute for Sustainable Malaria Control, University of Pretoria, Hatfield, Pretoria, 0028, South Africa

Mariette van der Watt – Department of Biochemistry, Genetics and Microbiology, Institute for Sustainable Malaria Control, University of Pretoria, Hatfield, Pretoria, 0028, South Africa; orcid.org/0000-0002-9933-8647

Dina Coertzen – Department of Biochemistry, Genetics and Microbiology, Institute for Sustainable Malaria Control, University of Pretoria, Hatfield, Pretoria, 0028, South Africa; orcid.org/0000-0002-8408-244X

Natasa Efstathiou – Laboratory of Medicinal Chemistry, Section of Pharmaceutical Chemistry, Department of Pharmacy, National and Kapodistrian University of Athens, Panepistimiopolis-Zografou, Athens 15771, Greece

Maria Chountoulesi – Section of Pharmaceutical Technology, Faculty of Pharmacy, National and Kapodistrian University of Athens, Panepistimiopolis-Zografou, Athens 15771, Greece

Carolyn M. Shoen – Central New York Research Corporation, Veterans Affairs Medical Center, Syracuse, NY 13210, USA; orcid.org/0000-0001-7627-3943

Ioannis P. Papanastasiou – Laboratory of Medicinal Chemistry, Section of Pharmaceutical Chemistry, Department of Pharmacy, National and Kapodistrian University of Athens, Panepistimiopolis-Zografou, Athens 15771, Greece; orcid.org/0000-0001-6974-2561

Jose Brea − Drug Screening Platform/Biofarma Research Group, CIMUS Research Center, Departamento de Farmacoloxía, Farmacia e Tecnoloxía Farmacéutica, University of Santiago de Compostela (USC), 15782 Santiago de Compostela, Spain; orcid.org/0000-0002-5523-1979;

Michael H. Cynamon − Central New York Research Corporation, Veterans Affairs Medical Center, Syracuse, NY 13210, USA; orcid.org/ 0000-0003-3796-9475

Lyn-Marié Birkholtz − Department of Biochemistry, Genetics and Microbiology, Institute for Sustainable Malaria Control, University of Pretoria, Hatfield, Pretoria, 0028, South Africa; orcid.org/0000-0001-5888-2905

Laurent Kremer - Centre National de la Recherche Scientifique UMR 9004, Institut de Recherche en Infectiologie de Montpellier (IRIM), Université de Montpellier, 1919 route de Mende, 34293, Montpellier, France ; orcid.org/0000-0002-6604-4458

Joo Hwan No − Leishmania Research Laboratory, Institut Pasteur Korea, Seongnam-si, Korea; orcid.org/0000-0002-3896-9808

Santiago Vázquez − Laboratori de Química Farmacèutica (Unitat Associada al CSIC), Departament de Farmacologia, Toxicologia i Química Terapèutica, Facultat de Farmàcia i Ciències de l'Alimentació, and Institute of Biomedicine (IBUB), Universitat de Barcelona, Av. Joan XXIII, 27-31, Barcelona, E-08028, Spain; orcid.org/0000-0002-9296-6026

Costas Demetzos − Section of Pharmaceutical Technology, Faculty of Pharmacy, National and Kapodistrian University of Athens, Panepistimiopolis-Zografou, Athens 15771, Greece; orcid.org/0000-0001-9771-4314

Gustavo Benaim − Instituto de Estudios Avanzados, Caracas, Venezuela Instituto de Biología Experimental, Facultad de Ciencias, Universidad Central de Venezuela (UCV), Caracas, Venezuela; orcid.org/ 0000-0002-9359-5546

Helen I. Zgurskaya − University of Oklahoma, Department of Chemistry and Biochemistry, Stephenson Life Sciences Research Center, 101 Stephenson Parkway, Norman, OK 73019-5251, USA; orcid.org/ 0000-0001-8929-4727

Thomas Dick − Center for Discovery and Innovation, Hackensack Meridian Health, Nutley, NJ 07110, USA; Department of Medical Sciences, Hackensack Meridian School of Medicine, Nutley, NJ 07110, USA; Department of Microbiology and Immunology, Georgetown University, Washington, DC 20007, USA; orcid.org/0000-0002-9604-9452

Author Contributions

†M.S. and S.R.M. contributed equally.

45

This research is part of MS Ph.D thesis. ADK conceived the project. ADK, MS designed, and MS synthesized and characterized the compounds. MM and SOB in HIZ lab performed binding assays. SRM and ZG performed testing against *M. smegmatis*, *B. subtilis* and *E. coli* in EO lab. AR-C, MV-D in GB lab performed testing against *L. mexicana*. NN and MC ran the DSC experiments, reported and interpreted the results in CD lab. A-LT performed the HRMS experiments and interpreted the results with SV. K-HB, T-NP, HL and JHN performed testing against *T. brucei*, *T. cruzi* and *L. donovani*. Alcohol **5i** was produced by NE and IPP. MHC designed and CMS performed testing against MtbErdman and MtbH37Rv. NA-C and TD determined activity against Mtb HN878. SW, MvdW and DC performed testing against *P. falciparum* parasites and HepG2 assays in L-MB lab. LK conceived experiments and analyzed data. MA performed experiments and analyzed data. JB carried out microsomal stability and solubility studies and wrote the results with SV. ADK, EO, MS, and SRM interpreted results and wrote the manuscript with all co-authors involved in the final editing of the paper.

Abbreviations Used

Bs, Bacillus subtilis; cryo-EM, cryogenic electron microscopy, DSC, differential scanning calorimetry; DEAD, diethyl azodicarboxylate; DFT, Density Functional Theory; DMPC, 1,2-dimyristoyl-sn-glycero-3-phosphocholine; DSPG, 1,2-distearoyl-sn-glycero-3-phosphoglycerol; *Ec, Eschericha coli;* esp = α,α,α′,α′-tetramethyl-1,3-benzenedipropionic acid; GAFF, Generalized Amber Force Field; HepG2, hepatocyte carcinoma; HOSA, hydroxylamine-O-sulfonic acid; HFIP, hexafluoroisopropanol; HRMS, High-resolution mass spectrometry; TB, Tuberculosis; *Mtb, Mycobacterium tuberculosis*; MDR, multi drug-resistant; XDR, extensively drug-resistant; MmpL3, mycobacterium membrane protein large 3; *Ms, Mycobacterium smegmatis; MtE, M.tuberculosis* Erdman; *MtHN878, M. tuberculosis* HN878; OPM, Orientations of Proteins in Membranes; PBS, phosphate buffer solution; POPC, 1-palmitoyl-2-oleoyl-sn-glycero-3-phosphocholine; RMSD, root mean square deviation; TMM, trehalose monomycolate; PMF, Proton motive force; RMSD, root-mean-square deviation; rt, room temperature; SID, simulation interaction diagram; THF, tetrahydrofuran; *T. brucei, Trypanosoma brucei; T. cruzi, Trypanosoma cruzi*.

Notes

The authors declare no competing financial interest.

ACKNOWLEDGEMENTS

REFERENCES

1. Walker, T. M.; Miotto, P.; Köser, C. U.; Fowler, P. W.; Knaggs, J.; Iqbal, Z.; Hunt, M.; Chindelevitch, L.; Farhat, M.; Cirillo, D. M.; Comas, I.; Posey, J.; Omar, S. V.; Peto, T. E.; Suresh, A.; Uplekar, S.; Laurent, S.; Colman, R. E.; Nathanson, C. M.; Zignol, M.; Walker, A. S.; Crook, D. W.; Ismail, N.; Rodwell, T. C., The 2021 WHO catalogue of Mycobacterium tuberculosis complex mutations associated with drug resistance: A genotypic analysis. *Lancet Microbe* **2022,** *3* (4), e265-e273.

2. Almeida Da Silva, P. E.; Palomino, J. C., Molecular basis and mechanisms of drug resistance in Mycobacterium tuberculosis: classical and new drugs. *J Antimicrob Chemother* **2011,** *66* (7), 1417-30.

3. Vasava, M. S.; Nair, S. G.; Rathwa, S. K.; Patel, D. B.; Patel, H. D., Development of new drug-regimens against multidrug-resistant tuberculosis. *Indian J Tuberc* **2019,** *66* (1), 12-19.

4. Lee, R. E.; Protopopova, M.; Crooks, E.; Slayden, R. A.; Terrot, M.; Barry, C. E., 3rd, Combinatorial lead optimization of [1,2]-diamines based on ethambutol as potential antituberculosis preclinical candidates. *J Comb Chem* **2003,** *5* (2), 172-87.

5. Heinrich, N.; Dawson, R.; du Bois, J.; Narunsky, K.; Horwith, G.; Phipps, A. J.; Nacy, C. A.; Aarnoutse, R. E.; Boeree, M. J.; Gillespie, S. H.; Venter, A.; Henne, S.; Rachow, A.; Phillips, P. P.; Hoelscher, M.; Diacon, A. H., Early phase evaluation of SQ109 alone and in combination with rifampicin in pulmonary TB patients. *J Antimicrob Chemother* **2015,** *70* (5), 1558-66.

6.   Sacksteder, K. A.; Protopopova, M.; Barry, C. E., 3rd; Andries, K.; Nacy, C. A., Discovery and development of SQ109: a new antitubercular drug with a novel mechanism of action. *Future Microbiol* **2012,** *7* (7), 823-37.

7.   Li, W.; Upadhyay, A.; Fontes, F. L.; North, E. J.; Wang, Y.; Crans, D. C.; Grzegorzewicz, A. E.; Jones, V.; Franzblau, S. G.; Lee, R. E.; Crick, D. C.; Jackson, M., Novel insights into the mechanism of inhibition of MmpL3, a target of multiple pharmacophores in Mycobacterium tuberculosis. *Antimicrob Agents Chemother* **2014,** *58* (11), 6413-23.

8.   Tahlan, K.; Wilson, R.; Kastrinsky, D. B.; Arora, K.; Nair, V.; Fischer, E.; Barnes, S. W.; Walker, J. R.; Alland, D.; Barry, C. E., 3rd; Boshoff, H. I., SQ109 targets MmpL3, a membrane transporter of trehalose monomycolate involved in mycolic acid donation to the cell wall core of Mycobacterium tuberculosis. *Antimicrob Agents Chemother* **2012,** *56* (4), 1797-809.

9.   Zhang, B.; Li, J.; Yang, X.; Wu, L.; Zhang, J.; Yang, Y.; Zhao, Y.; Zhang, L.; Yang, X.; Yang, X.; Cheng, X.; Liu, Z.; Jiang, B.; Jiang, H.; Guddat, L. W.; Yang, H.; Rao, Z., Crystal Structures of Membrane Transporter MmpL3, an Anti-TB Drug Target. *Cell* **2019,** *176* (3), 636-648.e13.

10.   Li, W.; Stevens, C. M.; Pandya, A. N.; Darzynkiewicz, Z.; Bhattarai, P.; Tong, W.; Gonzalez-Juarrero, M.; North, E. J.; Zgurskaya, H. I.; Jackson, M., Direct Inhibition of MmpL3 by Novel Antitubercular Compounds. *ACS Infect Dis* **2019,** *5* (6), 1001-1012.

11.   Li, K.; Schurig-Briccio, L. A.; Feng, X.; Upadhyay, A.; Pujari, V.; Lechartier, B.; Fontes, F. L.; Yang, H.; Rao, G.; Zhu, W.; Gulati, A.; No, J. H.; Cintra, G.; Bogue, S.; Liu, Y. L.; Molohon, K.; Orlean, P.; Mitchell, D. A.; Freitas-Junior, L.; Ren, F.; Sun, H.; Jiang, T.; Li, Y.; Guo, R. T.; Cole, S. T.; Gennis, R. B.; Crick, D. C.; Oldfield, E., Multitarget drug discovery for tuberculosis and other infectious diseases. *J Med Chem* **2014,** *57* (7), 3126-39.

12.   Onajole, O. K.; Belewa, X. V.; Coovadia, Y.; Govender, T.; Kruger, H. G.; Maguire, G. E. M.; Naidu, D.; Somai, B.; Singh, N.; Govender, P., SQ109 analogues as potential antimicrobial candidates. *Medicinal Chemistry Research* **2011,** *20* (8), 1394-1401.

13.   Makobongo, M. O.; Einck, L.; Peek, R. M., Jr.; Merrell, D. S., In vitro characterization of the anti-bacterial activity of SQ109 against Helicobacter pylori. *PLoS One* **2013,** *8* (7), e68917.

14.   Reader, J.; van der Watt, M. E.; Taylor, D.; Le Manach, C.; Mittal, N.; Ottilie, S.; Theron, A.; Moyo, P.; Erlank, E.; Nardini, L.; Venter, N.; Lauterbach, S.; Bezuidenhout, B.; Horatscheck, A.; van Heerden, A.; Spillman, N. J.; Cowell, A. N.; Connacher, J.; Opperman, D.; Orchard, L. M.; Llinás, M.; Istvan, E. S.; Goldberg, D. E.; Boyle, G. A.; Calvo, D.; Mancama, D.; Coetzer, T. L.; Winzeler, E. A.; Duffy, J.; Koekemoer, L. L.; Basarab, G.; Chibale, K.; Birkholtz, L. M., Multistage and transmission-

blocking targeted antimalarials discovered from the open-source MMV Pandemic Response Box. *Nat Commun* **2021,** *12* (1), 269.

15.   Veiga-Santos, P.; Li, K.; Lameira, L.; de Carvalho, T. M.; Huang, G.; Galizzi, M.; Shang, N.; Li, Q.; Gonzalez-Pacanowska, D.; Hernandez-Rodriguez, V.; Benaim, G.; Guo, R. T.; Urbina, J. A.; Docampo, R.; de Souza, W.; Oldfield, E., SQ109, a new drug lead for Chagas disease. *Antimicrob Agents Chemother* **2015,** *59* (4), 1950-61.

16.   Meng, Q.; Luo, H.; Chen, Y.; Wang, T.; Yao, Q., Synthesis of novel [1,2]-diamines with antituberculosis activity. *Bioorg Med Chem Lett* **2009,** *19* (18), 5372-5.

17.   Galaka, T.; Ferrer Casal, M.; Storey, M.; Li, C.; Chao, M. N.; Szajnman, S. H.; Docampo, R.; Moreno, S. N.; Rodriguez, J. B., Antiparasitic Activity of Sulfur- and Fluorine-Containing Bisphosphonates against Trypanosomatids and Apicomplexan Parasites. *Molecules* **2017,** *22* (1).

18.   Kolocouris, A.; Tzitzoglaki, C.; Johnson, F. B.; Zell, R.; Wright, A. K.; Cross, T. A.; Tietjen, I.; Fedida, D.; Busath, D. D., Aminoadamantanes with persistent in vitro efficacy against H1N1 (2009) influenza A. *J Med Chem* **2014,** *57* (11), 4629-39.

19.   Drakopoulos, A.; Tzitzoglaki, C.; McGuire, K.; Hoffmann, A.; Konstantinidi, A.; Kolokouris, D.; Ma, C.; Freudenberger, K.; Hutterer, J.; Gauglitz, G.; Wang, J.; Schmidtke, M.; Busath, D. D.; Kolocouris, A., Unraveling the Binding, Proton Blockage, and Inhibition of Influenza M2 WT and S31N by Rimantadine Variants. *ACS Med Chem Lett* **2018,** *9* (3), 198-203.

20.   Tzitzoglaki, C.; Drakopoulos, A.; Konstantinidi, A.; Stylianakis, I.; Stampolaki, M.; Kolocouris, A., Approaches to primary tert-alkyl amines as building blocks. *Tetrahedron* **2019,** *75* (34), 130408.

21.   Xie, J.; Si, X.; Gu, S.; Wang, M.; Shen, J.; Li, H.; Shen, J.; Li, D.; Fang, Y.; Liu, C.; Zhu, J., Allosteric Inhibitors of SHP2 with Therapeutic Potential for Cancer Treatment. *J Med Chem* **2017,** *60* (24), 10205-10219.

22.   Stampolaki, M.; Kolocouris, A., Improved Synthesis of the Antitubercular Agent SQ109. *SynOpen* **2021,** *05* (04), 321-326.

23.   Li, K.; Wang, Y.; Yang, G.; Byun, S.; Rao, G.; Shoen, C.; Yang, H.; Gulati, A.; Crick, D. C.; Cynamon, M.; Huang, G.; Docampo, R.; No, J. H.; Oldfield, E., Oxa, Thia, Heterocycle, and Carborane Analogues of SQ109: Bacterial and Protozoal Cell Growth Inhibitors. *ACS Infect Dis* **2015,** *1* (5), 215-221.

24.   Onajole, O. K.; Govender, P.; van Helden, P. D.; Kruger, H. G.; Maguire, G. E.; Wiid, I.; Govender, T., Synthesis and evaluation of SQ109 analogues as potential anti-tuberculosis candidates. *Eur J Med Chem* **2010,** *45* (5), 2075-9.

25.   Raynaud, C.; Daher, W.; Johansen, M. D.; Roquet-Banères, F.; Blaise, M.; Onajole, O. K.; Kozikowski, A. P.; Herrmann, J. L.; Dziadek, J.; Gobis, K.; Kremer, L., Active Benzimidazole Derivatives Targeting the MmpL3 Transporter in Mycobacterium abscessus. *ACS Infect Dis* **2020,** *6* (2), 324-337.

26.   Malwal, S. R.; Zimmerman, M. D.; Alvarez, N.; Sarathy, J. P.; Dartois, V.; Nacy, C. A.; Oldfield, E., Structure, In Vivo Detection, and Antibacterial Activity of Metabolites of SQ109, an Anti-Infective Drug Candidate. *ACS Infect Dis* **2021,** *7* (8), 2492-2507.

27.   Johansen, M. D.; Herrmann, J. L.; Kremer, L., Non-tuberculous mycobacteria and the rise of Mycobacterium abscessus. *Nat Rev Microbiol* **2020,** *18* (7), 392-407.

28.   Dupont, C.; Viljoen, A.; Dubar, F.; Blaise, M.; Bernut, A.; Pawlik, A.; Bouchier, C.; Brosch, R.; Guérardel, Y.; Lelièvre, J.; Ballell, L.; Herrmann, J. L.; Biot, C.; Kremer, L., A new piperidinol derivative targeting mycolic acid transport in Mycobacterium abscessus. *Mol Microbiol* **2016,** *101* (3), 515-29.

29.   García-García, V.; Oldfield, E.; Benaim, G., Inhibition of Leishmania mexicana Growth by the Tuberculosis Drug SQ109. *Antimicrob Agents Chemother* **2016,** *60* (10), 6386-9.

30.   Gil, Z.; Martinez-Sotillo, N.; Pinto-Martinez, A.; Mejias, F.; Martinez, J. C.; Galindo, I.; Oldfield, E.; Benaim, G., SQ109 inhibits proliferation of Leishmania donovani by disruption of intracellular Ca(2+) homeostasis, collapsing the mitochondrial electrochemical potential ($\Delta\Psi(m)$) and affecting acidocalcisomes. *Parasitol Res* **2020,** *119* (2), 649-657.

31.   Delcour, A. H., Outer membrane permeability and antibiotic resistance. *Biochim Biophys Acta* **2009,** *1794* (5), 808-16.

32.   Clifton, L. A.; Skoda, M. W.; Daulton, E. L.; Hughes, A. V.; Le Brun, A. P.; Lakey, J. H.; Holt, S. A., Asymmetric phospholipid: lipopolysaccharide bilayers; a Gram-negative bacterial outer membrane mimic. *J R Soc Interface* **2013,** *10* (89), 20130810.

33.   Feng, X.; Zhu, W.; Schurig-Briccio, L. A.; Lindert, S.; Shoen, C.; Hitchings, R.; Li, J.; Wang, Y.; Baig, N.; Zhou, T.; Kim, B. K.; Crick, D. C.; Cynamon, M.; McCammon, J. A.; Gennis, R. B.; Oldfield, E., Antiinfectives targeting enzymes and the proton motive force. *Proc Natl Acad Sci U S A* **2015,** *112* (51), E7073-82.

34.   Chiu, M. H.; Prenner, E. J., Differential scanning calorimetry: An invaluable tool for a detailed thermodynamic characterization of macromolecules and their interactions. *J Pharm Bioallied Sci* **2011,** *3* (1), 39-59.

35.   McMullen, T. P.; Lewis, R. N.; McElhaney, R. N., Calorimetric and spectroscopic studies of the effects of cholesterol on the thermotropic phase behavior and organization of a homologous series

of linear saturated phosphatidylglycerol bilayer membranes. *Biochim Biophys Acta* **2009,** *1788* (2), 345-57.

36.   Cong, W.; Liu, Q.; Liang, Q.; Wang, Y.; Luo, G., Investigation on the interactions between pirarubicin and phospholipids. *Biophysical Chemistry* **2009,** *143* (3), 154-160.

37.   Rowat, A. C.; Keller, D.; Ipsen, J. H., Effects of farnesol on the physical properties of DMPC membranes. *Biochimica et Biophysica Acta (BBA) - Biomembranes* **2005,** *1713* (1), 29-39.

38.   Chapman, D.; Urbina, J., Biomembrane phase transitions. Studies of lipid-water systems using differential scanning calorimetry. *J Biol Chem* **1974,** *249* (8), 2512-21.

39.   Jia, L.; Tomaszewski, J. E.; Hanrahan, C.; Coward, L.; Noker, P.; Gorman, G.; Nikonenko, B.; Protopopova, M., Pharmacodynamics and pharmacokinetics of SQ109, a new diamine-based antitubercular drug. *Br J Pharmacol* **2005,** *144* (1), 80-7.

40.   Jia, L.; Noker, P. E.; Coward, L.; Gorman, G. S.; Protopopova, M.; Tomaszewski, J. E., Interspecies pharmacokinetics and in vitro metabolism of SQ109. *Br J Pharmacol* **2006,** *147* (5), 476-85.

41.   Baek, K. H.; Phan, T. N.; Malwal, S. R.; Lee, H.; Li, Z. H.; Moreno, S. N. J.; Oldfield, E.; No, J. H., In Vivo Efficacy of SQ109 against Leishmania donovani, Trypanosoma spp. and Toxoplasma gondii and In Vitro Activity of SQ109 Metabolites. *Biomedicines* **2022,** *10* (3).

42.   de Bruyn Kops, C.; Stork, C.; Šícho, M.; Kochev, N.; Svozil, D.; Jeliazkova, N.; Kirchmair, J., GLORY: Generator of the Structures of Likely Cytochrome P450 Metabolites Based on Predicted Sites of Metabolism. *Front Chem* **2019,** *7*, 402.

43.   Stork, C.; Embruch, G.; Šícho, M.; de Bruyn Kops, C.; Chen, Y.; Svozil, D.; Kirchmair, J., NERDD: a web portal providing access to in silico tools for drug discovery. *Bioinformatics* **2020,** *36* (4), 1291-1292.

44.   Zaretzki, J.; Matlock, M.; Swamidass, S. J., XenoSite: accurately predicting CYP-mediated sites of metabolism with neural networks. *J Chem Inf Model* **2013,** *53* (12), 3373-83.

45.   Rydberg, P.; Gloriam, D. E.; Zaretzki, J.; Breneman, C.; Olsen, L., SMARTCyp: A 2D Method for Prediction of Cytochrome P450-Mediated Drug Metabolism. *ACS Med Chem Lett* **2010,** *1* (3), 96-100.

46.   Leshabane, M.; Dziwornu, G. A.; Coertzen, D.; Reader, J.; Moyo, P.; van der Watt, M.; Chisanga, K.; Nsanzubuhoro, C.; Ferger, R.; Erlank, E.; Venter, N.; Koekemoer, L.; Chibale, K.; Birkholtz, L. M., Benzimidazole Derivatives Are Potent against Multiple Life Cycle Stages of Plasmodium falciparum Malaria Parasites. *ACS Infect Dis* **2021,** *7* (7), 1945-1955.

47. Verlinden, B. K.; Niemand, J.; Snyman, J.; Sharma, S. K.; Beattie, R. J.; Woster, P. M.; Birkholtz, L. M., Discovery of novel alkylated (bis)urea and (bis)thiourea polyamine analogues with potent antimalarial activities. *J Med Chem* **2011,** *54* (19), 6624-33.

48. Grzegorzewicz, A. E.; de Sousa-d'Auria, C.; McNeil, M. R.; Huc-Claustre, E.; Jones, V.; Petit, C.; Angala, S. K.; Zemanová, J.; Wang, Q.; Belardinelli, J. M.; Gao, Q.; Ishizaki, Y.; Mikušová, K.; Brennan, P. J.; Ronning, D. R.; Chami, M.; Houssin, C.; Jackson, M., Assembling of the Mycobacterium tuberculosis Cell Wall Core. *J Biol Chem* **2016,** *291* (36), 18867-79.

49. Tikhonova, E. B.; Dastidar, V.; Rybenkov, V. V.; Zgurskaya, H. I., Kinetic control of TolC recruitment by multidrug efflux complexes. *Proc Natl Acad Sci U S A* **2009,** *106* (38), 16416-21.

Table of Contents Graphic

52